DOE/NASA/2593-18
NASA TM-81567

IMPROVED BOND COATINGS FOR USE WITH THERMAL BARRIER COATINGS

Michael A. Gedwill
National Aeronautics and Space Administration
Lewis Research Center

September 1980

Prepared for
U.S. DEPARTMENT OF ENERGY
Fossil Energy
Office of Coal Utilization

NOTICE

DOE/NASA/2593-18
NASA TM-81567

IMPROVED BOND COATINGS FOR USE WITH THERMAL BARRIER COATINGS

Michael A. Gedwill
National Aeronautics and Space Administration
Lewis Research Center
Cleveland, Ohio 44135

September 1980

Work performed for
U.S. DEPARTMENT OF ENERGY
Fossil Energy
Office of Coal Utilization
Washington, D.C. 20545
Under Interagency Agreement EF-77-A-01-2593

IMPROVED BOND COATINGS FOR USE WITH THERMAL BARRIER COATINGS

Michael A. Gedwill
National Aeronautics and Space Administration
Lewis Research Center
Cleveland, Ohio 44135

E-532

SUMMARY

A study was begun to identify those NiCrAl and CoCrAl bond coatings with the capability to improve the durability of thermal barrier coatings (TBC's) for potential use in gas turbines firing coal-derived fuels. Selected bond coatings alone were deposited on B-1900 + Hf and MAR-M-509 specimens and were screened for their oxidation resistance in cyclic furnace tests at 1000° and 1100° C. The performance of a ZrO_2-12Y_2O_3 TBC over several bond coatings was also evaluated in cyclic furnace endurance tests at 1010° C. The TBC and bond coatings were plasma deposited, except for two bond coatings that were sputter deposited. Failure of the TBC was considered to have occurred when external cracking of the TBC was observed.

The oxidation behavior of the bond coatings was improved when the thickness of the NiCrAl coatings was increased from 0.010 cm to 0.015 cm and when the coatings were plasma deposited at 20 kW with argon - 3.5-vol% hydrogen arc gas rather than at 11 kW with argon. The most oxidation resistant bond coatings were Ni-14.1Cr-13.4Al-0.10Zr, Ni-14.3Cr-14.4Al-0.16Y, and Ni-15.8Cr-12.8Al-0.36Y on B-1900 + Hf and Ni-30.9Cr-11.1Al-0.48Y on MAR-M-509. Bond coating oxidation resistance was sensitive to yttrium content, with high levels giving inferior performance.

The more oxidation resistant bond coatings greatly improved the life of the TBC when the coatings were plasma deposited on test specimens supported on a nail bed fixture during coating. TBC failure seemed to originate from microcracks within the TBC that formed near the plasma-deposited bond coating at the corners of the specimens.

It was also found that the bond coating must have sufficient surface roughness and good oxidation resistance in order for the TBC to have improved adherence and longevity. TBC life on relatively smooth, sputtered NiCrAlY and CoCrAlY bond coatings was relatively short as compared with TBC life on rougher, plasma-deposited bond coatings. When thin bond coatings were plasma deposited on the sputtered coatings (to give an intermediate roughness) significant life improvement occurred, but not to the same degree as with the more oxidation resistant, plasma-deposited bond coatings applied at 20 kW with argon - 3.5 vol% hydrogen.

INTRODUCTION

Improved gas turbine performance and fuel efficiency are obtained by increasing turbine inlet temperature. Thermally insulating thermal barrier coatings (TBC's) are actively being considered for application to the outer surfaces of cooled turbine blades and vanes so as to provide one possible way for engines to operate at higher inlet temperatures. Other nearer term benefits of using TBC's, however, are reductions in coolant flow and/or metal temperature. Since metal temperature reductions of at least 100 deg C can be realized by using these coatings, significant improvements in hot-

section durability can be attained. For these reasons TBC's are being developed for both aircraft and ground-power gas turbines that use relatively clean fuels (refs. 1 to 8), as well as for industrial and utility turbines that use dirty fuels (refs. 9 to 12).

The current interest in TBC's was sparked by the encouraging results obtained at NASA Lewis on the performance of TBC's on airfoil turbine alloys in furnace and Mach 1.0 burner rig endurance tests and in an aircraft research engine ground test (refs. 4 and 5). The best performance was achieved by a plasma-deposited, two-layer TBC system consisting of a 0.025- to 0.064-cm-thick ZrO_2-12Y_2O_3 top coating on a 0.003- to 0.008-cm-thick Ni-16.2Cr-5.6Al-0.61Y bond coating. (All compositions are expressed in weight percent.) More recent results of cyclic furnace, torch, and Mach 1.0 burner rig tests (ref. 7) have indicated that the performance and adherence of the two-layer TBC system can be substantially improved by adjusting the compositions of both the TBC and the bond coating. For example, a ZrO_2-7.9Y_2O_3 TBC and Ni-17.0Cr-5.4Al-0.35Y bond coating survived 2000 1-hr cycles in a natural-gas-fired Mach 1.0 burner rig at 1470° C surface temperature. Very recently a study involving cyclic furnace tests (ref. 8) reported other bond coating compositions that further improved the performance and adherence of a TBC. In that study it was found that a Ni-25.7Cr-5.6Al-0.32Y bond coating was the best of a limited number studied for ZrO_2-based TBC's. It was also suggested that adherence of a TBC strongly depends on the oxidation resistance of the bond coating and on chemical-electrostatic bonding between the TBC and the bond coating. Early TBC failures were observed when bond coatings with relatively poor oxidation resistance were employed. In these cases the bond coatings were completely oxidized.

The first-generation TBC system developed for clean-fuel-fired engines cracked and spalled very early in Mach 0.3 burner rig tests when simulated utility fuels were fired (ref. 10). For example, when the ZrO_2-12Y_2O_3/Ni-16.2Cr-5.6Al-0.61Y TBC system was tested at a surface temperature of 982° C and a metal substrate temperature of 843° C in Jet A combustion gases containing an intentionally added fuel equivalence of 5-ppm sodium plus 2-ppm vanadium, the ceramic spalled after only forty-three 1-hr cycles. The early failure was not attributed to a reaction between the fuel impurities and the bond coating, but rather to condensation of fuel impurities within the ceramic (ref. 11). It has also been shown (refs. 10 and 12), however, that bond coatings and ceramic compositions play important roles in determining TBC life in dirty fuels and that substantial life improvements are possible with improved compositions.

The present study was undertaken to identify bond coatings with the potential to improve the resistance of TBC's to the severe gas turbine environments expected in the combustion products of minimally processed petroleum or coal-derived fuels. The purpose was to identify bond coatings that would provide better TBC adherence. The study was supported by the U.S. Department of Energy (DOE), Office of Fossil Energy Programs, under Interagency Agreement EF-77-A-01-2593. Cyclic furnace oxidation was used as a first step to screen selected bond coatings that were plasma deposited on representative nickel- and cobalt-based turbine airfoil alloys. The effects of bond coating thickness (0.010 and 0.015 cm), plasma-deposition power (11 to 24 kW), and hydrogen additions to the argon plasma arc gas (0 and 3.5-vol% H_2 in argon) were investigated. The oxidation resistance of the bond coatings was judged on the basis of weight-change data, X-ray diffraction data, and metallographic analyses. The performance of a

ZrO_2-12Y_2O_3 TBC on several bond coatings was also evaluated in cyclic furnace endurance tests. All the TBC and bond coatings were plasma deposited, except for two bond coatings that were sputter deposited. TBC performance was judged by resistance to cracking and adherence. Weight-change data were obtained and post-test metallographic analyses were carried out to determine the oxidation behavior of the bond coatings in the presence of the TBC.

MATERIALS, APPARATUS, AND PROCEDURES

In this study a ZrO_2-12Y_2O_3 thermal barrier coating and various bond coatings were plasma deposited on rectangular test specimens of two cast nickel- and cobalt-based superalloys, B-1900 + Hf and MAR-M-509, respectively. (Two additional bond coatings, however, were sputter deposited on several specimens.) The chemical compositions of the plasma spray powders (all -200 +325 mesh) and the superalloy substrates are listed in table I. The dimensions of the bond coating oxidation specimens and the TBC endurance specimens were 2.5 cm by 1.9 cm by 0.5 cm and 2.5 cm by 2.5 cm by 0.5 cm, respectively. The edges and corners of all specimens were rounded to a radius of about 0.2 cm.

The general procedures used for specimen preparation and plasma coating deposition were the same as reported by Stecura (ref. 5). Exceptions to these procedures are presented in table II. The coatings were manually applied to a target thickness of either 0.010 or 0.015 cm for the bond coatings and 0.038 cm for the TBC. Each coating thickness was determined from measurements (using vernier calipers) taken before and after completely coating each specimen. The thickness values reported herein are averages of the maximum values for each major surface.

Cyclic furnace oxidation tests at 1000° and 1100° C (±2 deg C) were used to screen the bond coatings. Each cycle consisted of 1 hr in the hot zone followed by at least 20 min out of the furnace. The apparatus used is described in reference 13. During testing the specimens were suspended in platinum wire baskets, and weight changes were obtained periodically at room temperature. The oxidation resistance of the bond coatings was judged on the basis of weight-change data and results of post-test X-ray diffraction (XRD) and metallographic analyses.

The performance of the ZrO_2-12Y_2O_3 TBC on various bond coatings was evaluated in cyclic furnace endurance tests at 1010° C ±20 deg C. Except for inspections each cycle consisted of a 6-minute heatup, 60 minutes at 1010° C, and 60 minutes of cooling to 380° C. The cycle was similar to the cycle used by Stecura (ref. 5), and the same type of furnace was employed. For inspections the furnace power was shut off and the specimens were removed at temperatures of 100° C or less, weighed at room temperature, and then inspected for cracking. TBC performance was judged on the basis of resistance to cracking and adherence. Time to failure of the TBC was defined as the number of cycles to the first external crack observed in the TBC at 10X magnification. Testing was conducted for up to 1500 hr or until the second external crack was observed. Post-test metallographic analysis was conducted to determine the cracking mode, any loss in adherence of the TBC, and the extent of oxidation of the bond coating.

RESULTS AND DISCUSSION

Six plasma-deposited bond coatings were selected for this study:

I. Ni-16Cr-6Al-0.6Y
II. Ni-18Cr-12Al-0.6Y
III. Ni-31Cr-11Al-0.6Y
IV. Co-20Cr-10Al-0.6Y
V. Ni-14Cr-14Al-0.1Zr
VI. Ni-14Cr-14Al-0.1Y

Bond coating I was selected as the reference coating based on the work of Stecura (ref. 5). Bond coating II, with its higher aluminum content, is similar to overlay coatings now used to protect gas turbine hot-section hardware from oxidation. Bond coating III was reported to have very good oxidation and hot corrosion resistance (refs. 14 and 15). Bond coating IV was selected because CoCrAlY alloys are more hot corrosion resistant than NiCrAlY alloys. The yttrium content of the first four bond coatings was kept constant. As the study progressed, additional bond coatings (primarily having lower Y contents) became available. Recently a Ni-14Cr-14Al alloy containing 0.1 Zr was reported to possess exceptionally good resistance to oxidation (ref. 16). Therefore bond coatings of Ni-14Cr-14Al-0.1Zr (V) and Ni-14Cr-14Al-0.1Y (VI) were also included in this study.

Tables III and IV list the results of the cyclic oxidation studies at 1000° and 1100° C of various plasma-deposited bond coatings on B-1900 + Hf and MAR-M-509, respectively. The optimum oxidation behavior can be characterized by a low positive weight change caused by the formation of a thin, stable protective oxide; a very low positive or zero slope of the oxidation-weight-change-versus-time curve once the oxide is formed; and finally the absence of oxide spalling and/or vaporization. The bond-coating final oxidation data listed in tables III and IV are the specific weight change and the slope of the weight-change-versus-time curve at the conclusion of testing. As discussed later the oxidation behavior of the bond coatings was found to be greatly influenced not only by exposure temperature and substrate composition, but also by coating-thickness and plasma-deposition conditions.

B-1900 + Hf Substrates

0.010-cm-thick bond coatings. - Weight change results for furnace tests of various 0.010-cm-thick bond coatings on B-1900 + Hf at 1000° and 1100° C are shown in figure 1. The bond coatings were plasma deposited at 11 kW with argon (baseline conditions). All nickel-based bond coatings can be considered oxidation resistant at 1000° C (fig. 1(a)) since they are still slowly gaining weight at 1200 hr. The XRD data in table III, however, suggest that the Ni-18.0Cr-11.9Al-0.55Y and Ni-16.2Cr-5.6Al-0.61Y bond coatings were the least oxidation resistant since the major oxides formed, NiO or Cr_2O_3, are less protective than α-Al_2O_3 and/or $NiAl_2O_4$ (refs. 17 to 19). The major oxides formed on the other three nickel-based bond coatings were α-Al_2O_3 and/or $NiAl_2O_4$. However, post-test metallographic examination of the cross sections of the specimens with the nickel-based coatings revealed no significant differences, except that the Ni-30.9Cr-11.1Al-0.48Y bond coating was slightly more oxidized. Based on

all these results the Ni-17.7Cr-12.2Al-0.11Y and Ni-14.1Cr-13.4Al-0.10Zr coatings appear to be most oxidation resistant when deposited under the baseline conditions described previously. In comparison the cobalt-based coating had poor oxidation resistance based on observed severe spalling (i.e., large weight loss) after about 800 hr.

Since the weight-change behavior of the nickel-based bond coatings was about the same throughout the 1200-hr test at 1000° C, all bond coatings were also evaluated at 1100° C. Comparison of figures 1(a) and (b) indicates that the oxidation behavior of the bond coatings was very sensitive to test temperature. Increasing the temperature from 1000° C to 1100° C reduced the oxidation resistance of the bond coatings (based on the time to exhibit a loss in weight) by over a factor of 6. The results in figure 1(b) also show that at 1100° C, as expected, the cobalt-based bond coating again had poorer oxidation resistance relative to the nickel-based bond coatings. Also, of the nickel-based bond coatings, the reference Ni-16.2Cr-5.6Al-0.61Y coating had the highest initial rate of weight pickup, suggesting that it has lower oxidation resistance than the other five nickel-based coatings. For these reasons, the cobalt-based and the reference nickel-based coatings were eliminated from further testing on B-1900 + Hf. Of this group the bond coating with the best oxidation resistance at 1100° C based on weight change versus time was Ni-17.7Cr-12.2Al-0.11Y; all other bond coatings began to lose weight as a result of severe spalling in less than 200 hr. Note that as in figure 1(b) two other nickel-based bond coatings have about the same chromium and aluminum contents as the Ni-17.7Cr-12.2Al-0.11Y coating, but higher yttrium contents (i.e., 0.36 and 0.55 weight percent). Comparison of the weight-change behavior of these three bond coatings shows that the time to onset of severe spalling increases as the yttrium content decreases. Stecura in a similar manner observed that the life of a TBC increased as the yttrium content in Ni-16Cr-5Al-xY bond coatings was decreased from 1.08 to 0.15 weight percent (ref. 7). These observations can be attributed to the effect of yttrium on bond coating oxidation resistance, as shown in figure 1(b). In the 1100° C oxidation tests the less desirable $NiAl_2O_4$ spinel rather than α-Al_2O_3 was the generally predominant oxide after 200 hr (table III).

Metallographic cross sections of the Ni-17.7Cr-12.2Al-0.11Y bond coating on B-1900 + Hf are shown in figure 2 in the as-deposited condition and after oxidation. Comparable amounts of oxidation of the coating occurred in the 1200-hr - 1000° C and 200-hr - 1100° C tests. After 200 hr at 1100° C the depleted zone of the substrate, however, is somewhat larger than after 1200 hr at 1000° C.

To determine the effects of plasma deposition power and hydrogen addition to the arc gas on the oxidation resistance of the bond coatings, four coatings (Ni-18.0Cr-11.9Al-0.55Y, Ni-15.8Cr-12.8Al-0.36Y, Ni-30.9Cr-11.1Al-0.48Y, and Ni-14.1Cr-13.4Al-0.10Zr) were plasma deposited at higher power levels with argon and argon - 3.5-vol% H_2. It was felt that increasing the power would increase the densities of the coatings and thereby afford improved oxidation resistance. It was also felt that the addition of hydrogen to the plasma gas would reduce spray-particle surface oxidation during passage through the plasma and while traveling to the substrate. Comparison of the 1100° C data for 0.010-cm-thick bond coatings in table III shows that increasing power in the range 11 to 17 kW with argon alone had very little to no beneficial effect on bond coating oxidation resistance. For example, Ni-15.8Cr-12.8Al-0.36Y exhibited a net weight loss

at 200 hr in all cases. However, the oxidation resistance of 0.010-cm-thick bond coatings was improved by deposition at 20 kW with argon - 3.5-vol% H_2. Now, for example, after 200 hr the specific weight change is positive for Ni-15.8Cr-12.8Al-0.36Y. For these latter deposition conditions the oxidation data (table III) indicate that Ni-30.9Cr-11.1Al-0.48Y and Ni-14.1Cr-13.4Al-0.10Zr were most resistant, but post-term metallographic examination indicated that Ni-15.8Cr-12.8Al-0.36Y and Ni-14.1Cr-13.4Al-0.10Zr were most resistant. These bond coatings suffered less oxidation than those shown in figure 2(c). The XRD data in table III show that the more desirable α-Al_2O_3 was one of the major oxides formed after 200 hr at 1100° C on Ni-30.9Cr-11.1Al-0.48Y and on Ni-14.1Cr-13.4Al-0.10Zr when deposited at 20 kW with argon - 3.5-vol% H_2. With the 11-kW/argon baseline conditions, the less desirable $NiAl_2O_4$ spinel was formed in greater quantity than α-Al_2O_3.

0.015-cm-thick bond coatings. - After metallographically examining numerous as-coated and oxidized specimens with 0.010-cm-thick plasma-deposited bond coatings, it became apparent that there were areas on the specimens that had a very thin coating or no coating at all. Stecura also observed thinly coated areas on specimens manually coated with less than 0.015-cm-thick bond coatings and found increases in thickness beneficial (ref. 8). As a result of these observations, coating thickness was increased by 50 percent to 0.015 cm for subsequent testing.

The 1100° C final oxidation data in table III show a definite improvement in oxidation resistance with an increase in coating thickness from 0.010 cm to 0.015 cm for the Ni-15.8Cr-12.8Al-0.36Y and Ni-17.7Cr-12.2Al-0.11Y bond coatings on B-1900 + Hf. These bond coatings were plasma deposited at 11 kW with argon. The predominant protective oxide on the thicker bond coatings was α-Al_2O_3 (table III) rather than $NiAl_2O_4$. Post-test metallography revealed that the thicker bond coatings were less oxidized and that the substrate depletion zone was thinner.

The improved oxidation resistance with an increase in coating thickness was more pronounced when bond coatings were applied at 14 kW, as shown in figure 3. In all three cases, the thicker coatings either did not begin to lose weight in the 200-hr test or weight loss began at a much later time. The predominant oxide formed on the two thicker bond coatings that did not begin to lose weight was again α-Al_2O_3. In contrast, the predominant oxide on the thicker Ni-18.0Cr-11.9Al-0.55Y bond coating, which began to lose weight, was $NiAl_2O_4$ spinel after 200-hr of oxidation. Metallographic cross sections of the two better bond coatings, figure 4, generally indicate less severe oxidation and substrate depletion when the thicker, 0.015-cm-thick bond coatings were tested.

The effects of plasma power and hydrogen additions to the arc gas on the 1100° C oxidation behavior of a 0.015-cm-thick Ni-15.8Cr-12.8Al-0.36Y bond coating on B-1900 + Hf are shown in figure 5. As is evident in this figure the oxidation resistance of the bond coating improved with increasing power in the range 11 to 17 kW when argon was used. Some additional improvement was realized when argon - 3.5-vol% H_2 was used at 16 and 20 kW. An exception to this trend was the observation that the oxidation resistance was somewhat less when the coating was applied at 24 kW than when it was applied at 20 kW. The XRD results (table III) and metallographic evaluations after test indicated no significant differences between the coatings deposited at 20 or 24 kW. The XRD results also indicated that generally α-Al_2O_3 was the predominant oxide. Post-test photomicrographs of bond coatings applied at 17 kW with argon and at 16 kW with argon - 3.5-vol% H_2

are shown in figure 6. A comparison of figures 6(a) and 4(a) reveals that the bond coating and the substrate were less oxidized and that substrate depletion was less severe when the coating was deposited at 17 kW with argon rather than at 14 kW with argon. Also, a comparison of figures 6(a) and (b) confirms that a little hydrogen in the arc gas improves the oxidation resistance of the bond coating. The coating applied at 16 kW with argon - 3.5-vol% H_2 exhibited a lesser amount of internal oxidation at 17 kW with argon alone and gave better protection to the substrate as indicated by the thinner depleted zone.

At this point in the present study it was felt that the plasma-deposition and coating-thickness parameters were optimized well enough to satisfactorily perform a final screening of oxidation resistance of the bond coatings. The bond coatings were plasma deposited at 20 kW with argon - 3.5-vol% H_2 arc gas to a nominal thickness of 0.015 cm. The results in figure 7 indicate that five of the bond coatings offered about equally good oxidation resistance on B-1900 + Hf at 1100° C. The other bond coating, Ni-18Cr-11.9Al-0.55Y, experienced eventual weight loss. After the 200-hr test XRD analysis of all six bond coatings showed α-Al_2O_3 as the predominant, or one of the predominant, oxides (table III).

Figure 8 shows cross-sectional microstructures of the bond coatings whose weight-change behavior was presented in figure 7. The microstructures of Ni-14.3Cr-14.4Al-0.16Y, Ni-14.1Cr-13.4Al-0.10Zr, and Ni-15.8Cr-12.8Al-0.36Y bond coatings appear to be the best, and very similar, after oxidation for 200 hr at 1100° C. The higher weight gains of Ni-14.1Cr-13.4Al-0.10Zr on B-1900 + Hf, shown in figure 7, are probably due to the observed slightly thicker surface oxide layer formed during oxidation. Because of the better overall microstructures after oxidation (fig. 8), the author believes that the most oxidation resistant bond coatings for B-1900 + Hf are Ni-14.3Cr-14.4Al-0.16Y, Ni-14.1Cr-13.4Al-0.10Zr, and Ni-15.8Cr-12.8Al-0.36Y even though this is not completely supported by the weight-change behavior (fig. 7).

As discussed previously the oxidation resistance of a 0.010-cm-thick Ni-17Cr-12Al-xY bond coating sprayed at 11 kW with argon arc gas was observed to decrease as the yttrium content increased from 0.11 wt% to 0.55 wt%. The data in figure 7, however, suggest that for at least 200 hr at 1100° C the oxidation resistance of this bond coating when sprayed at higher power with hydrogen in the arc gas to a thickness of 0.015 cm is unchanged when the yttrium content is increased from 0.11 wt% to 0.36 wt% but decreases when the yttrium content is increased to 0.55 wt%. However, comparison of figures 8(c), (d), and (e) indicates that an yttrium content of 0.36 wt% for a nominal Ni-17Cr-12Al-xY bond coating is better than 0.11 percent and much better than 0.55 percent. Similar results might be expected with a reduction of the yttrium content of Ni-30.9Cr-11.1Al-xY.

MAR-M-509 Substrates

0.010-cm-thick bond coatings. - Some of the bond coatings for initial testing on MAR-M-509 were plasma deposited to a nominal thickness of 0.010 cm at 11 kW with argon arc gas. The cyclic oxidation behavior of these coatings at 1000° and 1100° C is shown in figure 9. At 1000° C (fig. 9(a)) these coatings generally experienced higher weight gains after about 300 hr on MAR-M-509 than on B-900 + Hf (fig. 1(a)). This suggests that the bond coatings were less oxidation resistant on MAR-M-509, perhaps because of

diffusion of cobalt and maybe tungsten into the coatings. As noted previously for B-1900 + Hf, the cobalt-based bond coating also had poorer oxidation resistance than the nickel-based bond coating on MAR-M-509. Figure 9(a) indicates that the cobalt-based coating had the highest initial oxidation rate and that its weight gains were always above those of the nickel-based coatings throughout the 1200-hr test. The XRD data of table IV show that the major oxides after 1200 hr were either $NiCr_2O_4$, $CoCr_2O_4$, NiO, or Cr_2O_3, all of which are less protective than either α-Al_2O_3 and/or the spinels $NiAl_2O_4$ and $CoAl_2O_4$ (refs. 17 to 19). The only bond coating on MAR-M-509 that looked promising in 1000° C oxidation was Ni-30.9Cr-11.1Al-0.48Y. Post-test metallography, however, revealed that this coating was highly oxidized and that much of the oxide had apparently spalled off. Metallography of the other specimens tested at 1000° C also showed very severe oxidation of the bond coatings. The severity was much greater than that shown in figure 2(b) for a bond coating similarly applied and tested on B-1900 + Hf.

Oxidation was much more severe at 1100° C (fig. 9(b)) then at 1000° C. As in the case of B-1900 + Hf the oxidation resistance of the bond coatings on MAR-M-509 was also reduced by over a factor of 6 when the test temperature was increased. At 1100° C the only bond coating on MAR-M-509 that appeared to have some oxidation resistance up to 200 hr at 1100° C was Ni-15.8Cr-12.8Al-0.36Y, but its weight gain was considered high. The major oxide on this bond coating after 200 hr was $NiAl_2O_4$ and/or $CoAl_2O_4$ (table IV). All the other coatings started to spall within 125 hr as a result of severe oxidation. Post-test metallography of the Ni-15.8Cr-12.8Al-0.36Y bond coating, however, showed that the coating was severely oxidized and that some oxidation of the substrate had occurred. The degree of oxidation was much greater than that shown in figure 2(c) for a similarly applied and tested bond coating on B-1900 + Hf.

0.015-cm-thick bond coatings. - Although the effects of coating-thickness and plasma-deposition parameters were not as extensively investigated with MAR-M-509, the findings obtained were similar to those obtained with B-1900 + Hf. Increasing the coating thickness and/or the power during plasma deposition generally resulted in more oxidation resistant bond coatings on MAR-M-509 (table IV). These observations were supported by post-test metallographic evaluations.

Only the two bond coatings noted in the preceding section were plasma deposited on MAR-M-509 under conditions that were found to be about optimum and then tested for oxidation behavior at 1100° C. The coatings were applied to 0.015-cm thickness at 20 kW with argon - 3.5-vol% H_2 arc gas. The results, plotted in figure 10, indicate that Ni-30.9Cr-11.1Al-0.48Y is more oxidation resistant because it experienced a lower oxidation rate after about 10 hr and a lower weight gain after 200 hr than Ni-15.8Cr-12.8Al-0.36Y on MAR-M-509. The major oxides detected on both bond coatings after 200 hr were α-Al_2O_3 and $NiAl_2O_4$ and/or $CoAl_2O_4$ (table IV). However, these two bond coatings were more oxidation resistant on B-1900 + Hf than on MAR-M-509 when similarly applied (figs. 7 and 10). Both coatings generally experienced higher oxidation rates and weight gains on MAR-M-509 throughout the 200-hr test.

Figure 11 shows metallographic cross sections of the two bond coatings of figure 10 after oxidation at 1100° C. The microstructure of the Ni-30.9Cr-11.1Al-0.48Y bond coating (fig. 11(a)) indicates much less oxidation than that of the Ni-13.8Cr-12.8Al-0.36Y bond coating (fig. 11(b)). Also, the latter coating is considerably thinner, which indicates that it

experienced much more spalling during oxidation. Comparisons of these microstructures to those in figures 8(c) and (f) further illustrate the greater difficultly associated with protection of MAR-M-509 than B-1900 + Hf. Figures 11(a) and 8(f) suggest that the surface oxide layer is thicker and less tenacious on Ni-30.9Cr-11.1Al-0.48Y on MAR-M-509 and that this coating is slightly more oxidized on MAR-M-509 than on B-1900 + Hf. Figures 11(b) and 8(c) clearly show that the Ni-15.8Cr-12.8Al-0.36Y coating is considerably more oxidized on MAR-M-509 than on B-1900 + Hf.

TBC Cyclic Furnace Endurance

The performance of a ZrO_2-12Y_2O_3 TBC with various bond coatings on B-1900 + Hf and MAR-M-509 substrates was investigated in cyclic furnace endurance tests at 1010° C. Most of the specimens tested had plasma-deposited bond coatings; a few were tested with sputtered bond coatings. Initially, the tests were conducted for 750 hr or until the second external crack was observed at 10X magnification in the TBC (whichever came first). Later some of the specimens with the more oxidation resistant bond coatings were tested up to 1500 hr.

Plasma-deposited bond coatings. - The results obtained for the performance of the TBC in cyclic furnace endurance tests are summarized in figure 12. On B-1900 + Hf (fig. 12(a)) the 0.010-cm-thick Ni-15.8Cr-12.8Al-0.36Y and Ni-14.1Cr-13.4Al-0.10Zr bond coatings (plasma deposited at 11 kW with argon) appeared to significantly improve the life of the TBC relative to the reference Ni-16.2Cr-5.6Al-0.61Y bond coating. For the 0.010-cm-thick cobalt-based bond coating, Co-20.0Cr-9.1Al-0.63Y, however, only a slight improvement, if any, was observed in life over that of the reference bond coating on B-1900 + Hf. On MAR-M-509 (fig. 12(b)) the two bond coatings, Ni-30.9Cr-11.1Al-0.48Y and Co-20.0Cr-9.1Al-0.63Y, apparently gave shorter TBC life than the reference bond coating.

It is evident in figure 12 that there was considerable scatter in the TBC performance data obtained in this study, especially in the data shown for the 0.010-cm-thick bond coatings applied at 11 kW with argon. These bond coatings and the TBC were plasma deposited under the same conditions as reported by Stecura (ref. 5). There was less scatter observed by Stecura (private communication). One plausible reason for this is that in Stecura's studies the specimens were visually inspected for cracking, but in the present study inspections were made at 10X magnification using high-intensity illumination.

An example of a typical external crack on a tested specimen is shown in figure 13(a), and its cross section is presented in figure 13(b). The external cracks were always observed at the corners of the specimens. The cross sections of all the specimens tested revealed microcracks within the TBC at the corners, even in those specimens that did not exhibit external cracks after testing. If microcracking was relatively severe at the corners, the microcracks would extend completely around the cross sections and, in some instances, to the external surfaces either at about 90° or 45°. With plasma-deposited bond coatings the microcracks were always within the TBC and generally near the TBC - bond coating interfaces. Similar cracking was reported by Stecura (ref. 7) in furance and burner rig tests and by Levine (ref. 20) in adhesive-cohesive studies on plasma-deposited bond coatings and TBC's. From these observations it can be concluded that the external cracks observed are extensions of the microcracks formed at the corners of the specimens.

Metallographic examination of numerous specimens indicated that the thickness of the bond coating and the TBC could vary significantly around the corners of the specimens. This is perhaps another reason for the large data scatter in figure 12.

TBC performance was also obtained for some of the more oxidation resistant bond coatings identified previously. These bond coatings were plasma deposited at 20 kW with argon - 3.5-vol% H_2 to a nominal thickness of 0.015 cm. The TBC and bond coatings were both deposited while the B-1900 + Hf and MAR-M-509 specimens were being supported on a flat plate or on a nail bed fixture. Figure 14 shows a specimen on the nail bed fixture before coating. In another study the lives of TBC's were shown to be greatly improved when the specimens were coated while being supported on the nail bed fixture (unpublished data of R. A. Miller, NASA Lewis Research Center). In that study it was observed that "ricochet" spraying the under surface of the specimens, which produces a less dense deposit, was eliminated when the nail bed fixture was employed in place of a flat plate. As shown in figure 12 for the thicker, more oxidation resistant bond coatings, the life of the TBC on both substrates was significantly better when the coatings were applied while the substrates were supported on the nail bed fixture rather than on a flat plate. The two MAR-M-509 specimens (fig. 12(b)) coated on the nail bed fixture were tested for 1500 hr without exhibiting a second crack. The improved performance of the specimens coated on the nail bed fixture is attributed primarily to elimination of under spraying and secondarily to less oxidation of the bond coatings during deposition because of a lower substrate temperature. A matte-to-charcoal-grey-colored band was observed at the edges of one of the major surfaces after the bond coatings were applied to the specimens supported on a flat plate. Such a band was never observed when the specimens were coated on the nail bed fixture.

The weight-change behavior of thermal-barrier-coated specimens during cyclic furnace endurance testing is shown in figure 15. In general the specimens that were coated on a flat plate with 0.015-cm-thick bond coatings deposited at the improved deposition parameters unexpectedly exhibited about the same behavior (until testing was terminated) as the specimens with 0.010-cm-thick bond coatings deposited at the initial deposition parameters. The specimens coated on the nail bed fixture, however, showed weight gains that were definitely smaller. The weight-change behavior for the Ni-15.8Cr-12.8Al-0.36Y bond coating on B-1900 + Hf (not shown in fig. 15) was similar to that for the Ni-14.1Cr-13.4Al-0.10Zr bond coating on B-1900 + Hf in all cases. A comparison of figures 15(a) and (b) suggests that the Ni-30.9Cr-11.1Al-0.48Y bond coating on MAR-M-509 was less oxidation resistant than the Ni-14.1Cr-13.4Al-0.10Zr bond coating on B-1900 + Hf. After about 700 cycles the MAR-M-509 specimens experienced higher weight gains. This is in agreement with the findings discussed earlier. Also, the MAR-M-509 specimens coated on the nail bed fixture experienced an increasing oxidation rate after about 500 hr. This might explain why the MAR-M-509 specimens showed TBC cracking in less than 1500 hr but the B-1900 + Hf specimens did not (fig. 12).

Post-test photomicrographs of endurance-tested specimens are presented in figures 16 and 17. (Note that fig. 17(a) is the microstructure of a tested specimen after 750 hr rather than after 1500 hr.) The microstructures of the tested specimens with the 0.015-cm-thick bond coatings deposited at 20 kW with hydrogen added to the arc gas definitely appear better than those of the specimens with 0.010-cm-thick bond coatings deposited at 11 kW with argon only (compare figs. 16(a) and (b) after 1500 hr

and figs. 17(a) and (b) after 750 and 1500 hr, respectively). The 0.010-cm-thick bond coatings (figs. 16(a) and 17(a)) after test appear to consist of only a single metallic phase, whereas the thicker bond coatings (figs. 16(b) and 17(b)) have at least two metallic phases. From the Ni-Cr-Al ternary phase diagram (ref. 21), at least β (NiAl) and γ' (Ni_3Al) phases would be expected to be present in these two coatings when deposited under equilibrium conditions. (The Ni-30.9Cr-11.1Al-0.48Y coating would also be expected to contain a third phase, α-Cr.) During endurance testing and concurrent depletion of aluminum (by oxidation and/or diffusion into the substrate), β and later γ' would be lost and γ (Ni solid solution) would ultimately form. Furthermore figure 17(a) shows a region that apparently had no bond coating.

Bond coatings Ni-15.8Cr-12.8Al-0.36Y and Ni-30.9Cr-11.1Al-0.48Y have very recently been evaluated with TBC's on a nickel-based alloy (IN-792) in a Mach 0.3 burner rig at a surface temperature of 982° C (ref. 12). The bond coatings were plasma deposited at 11 kW with an argon arc gas. The burner rig was fired with Jet A fuel and the combustion gases contained an intentionally added fuel equivalence of 5-ppm sodium plus 2-ppm vanadium. The reported test results showed that these bond coatings essentially doubled the life of the TBC's (ZrO_2-$8Y_2O_3$ and/or Ca_2SiO_4) as compared with the "standard" Ni-15Cr-6Al-0.31Y bond coating. Further improvements are anticipated with the more oxidation resistant bond coatings plasma deposited at 20 kW with argon - 3.5-vol% H_2 arc gas.

Sputtered bond coatings. - To eliminate bond coating oxidation during plasma deposition and to determine TBC performance on more dense bond coatings, specimens of B-1900 + Hf and MAR-M-509 with sputtered 0.013-cm-thick Ni-15Cr-14Al-0.2Y and Co-19Cr-13Al-0.5Y bond coatings and plasma deposited ZrO_2-$12Y_2O_3$ TBC were endurance tested at 1010° C. Before the TBC was applied, the sputtered coatings were grit blasted with alumina to roughen the surfaces. This treatment increased the surface roughness from 0.9 μm to 2.5 μm (AA). However, the sputtered coatings after grit blasting were still relatively smooth as compared with the plasma-deposited coatings. The surface roughness of the latter coatings was in the range 7.6 to 12.7 μm (AA). Tucker, et al. (ref. 22) indicated that the bond coating must be rougher than 6.3 μm (AA) for improved adherence of the TBC. The TBC with the sputtered bond coatings cracked very early (<25 cycles) in the endurance test. In contrast, the TBC on the specimens with the plasma-deposited bond coatings generally exhibited much longer lives (fig. 12). Post-test metallography of the specimens with the sputtered bond coatings showed that TBC failure occurred essentially by interfacial separation of the TBC and the bond coatings, the separation being the greatest at the specimen corners. This behavior was similar to that observed by Stecura in testing TBC's applied directly to superalloy specimens (ref. 8).

To further increase the roughness of the sputtered bond coatings, and to see how well a dense, environmentally resistant sputtered base coating and a plasma-deposited bond coating/oxide top coating would perform, thin (0.003 to 0.006 cm) coatings were plasma deposited (at 11 kW with argon) on several alumina-blasted, sputter-coated specimens before the TBC was applied. The surface roughness of these duplex bond coatings was in the range of 5.6 to 8.4 μm (AA). The thin, plasma-deposited coatings deposited over the sputtered coatings greatly improved the life of the TBC. The specimens with the duplex bond coatings had TBC lives in the range 165 to 398 hr. This is more than a 500 percent increase over the lives of the specimens with only the sputtered bond coatings. The improved TBC lives with the

duplex bond coatings, however, were still significantly less than those of the specimens with the more oxidation resistant, plasma-deposited bond coatings. This may be due to the poor oxidation resistance of the added coating and/or the lower surface roughness. Post-test metallographic examination of the duplex-bond-coated specimens revealed that microcracking generally occurred within the TBC and very close to the TBC - bond coating interface. Based on these results it can be concluded that sufficient surface roughness and good oxidation resistance are both required of the bond coating for improved adherence and longevity of the TBC.

SUMMARY OF RESULTS

This study was conducted to identify bond coatings with potential for improving the durability of thermal barrier coatings (TBC's) to be used in gas turbine environments fired with coal-derived fuels. Cyclic furnace oxidation tests at 1000° and 1100° C were used to screen the bond coatings alone deposited on the nickel- and cobalt-based superalloys B-1900 + Hf and MAR-M-509, respectively. The effects of coating composition and thickness, plasma-deposition power, and hydrogen additions to the argon plasma arc gas were investigated. The oxidation resistance of the bond coatings was judged on the basis of weight-change data and results of post-test X-ray diffraction and metallographic analyses. The performance of a ZrO_2-12Y_2O_3 TBC with various bond coatings was evaluated in cyclic furnace endurance tests at 1010° C. The TBC and most of the bond coatings were plasma deposited; two bond coatings were sputter deposited. TBC performance was judged by its resistance to cracking and its adherence. Time of failure of the TBC was considered to be the number of cycles to the first external crack observed at 10X magnification. Weight-change data were obtained during endurance testing, and post-test metallographic analyses were conducted. The results from this study are as follows:

Oxidation of Plasma-Deposited Bond Coatings

1. The oxidation behavior of the bond coatings was improved significantly when the coating thickness was increased from 0.010 cm to 0.015 cm and the coatings were plasma deposited at 20 kW with argon - 3.5-vol% H_2 arc gas rather than at 11 kW with argon alone as the arc gas.

2. The most oxidation resistant bond coatings identified for B-1900 + Hf were Ni-14.1Cr-13.4Al-0.10Zr, Ni-14.3Cr-14.4Al-0.16Y, and Ni-15.8Cr-12.8Al-0.36Y. The reference bond coating (Ni-16.2Cr-5.6Al-0.61Y) as well as the only cobalt-based coating (Co-20.0Cr-9.1Al-0.63Y) investigated in this study both had poor oxidation resistance on B-1900 + Hf.

3. The oxidation resistance of a Ni-17Cr-12Al-xY bond coating on B-1900 + Hf was sensitive to the yttrium content. The coating containing 0.36Y was slightly more oxidation resistant than that containing 0.11Y and much more resistant than that containing 0.55Y when deposited at 20 kW with argon - 3.5-vol% H_2 arc gas. For the baseline deposition conditions of 11 kW with argon, oxidation resistance increased as the yttrium content decreased.

4. For MAR-M-509 the most oxidation resistant bond coating found was Ni-30.9Cr-11.1Al-0.48Y. The oxidation resistance of the Co-20.0Cr-9.1Al-0.63Y bond coating was poor as compared with the reference Ni-16.2Cr-5.6Al-0.61Y bond coating. On MAR-M-509 the reference bond coating was nearly as good as Ni-18.0Cr-11.9Al-0.55Y.

5. Oxidation behavior was very sensitive to test temperature. Increasing the temperature from 1000° C to 1100° C reduced the oxidation resistance of the bond coatings that were plasma deposited at 11 kW with argon by over a factor of 6.

6. α-Al_2O_3 was the predominant oxide or one of the predominant oxides formed on the more oxidation resistant bond coatings.

Endurance of TBC

7. The more oxidation resistant bond coatings as achieved through a combination of powder composition and deposition parameters (see results 3 and 4 above) greatly improved the life of the TBC when the bond coatings and TBC were plasma deposited on test specimens lying on a nail bed fixture rather than on a flat plate.

8. Sufficient surface roughness and good oxidation resistance are both required of the bond coating for improved adherence and longevity of the TBC. The TBC life for specimens with grit-blasted, sputtered NiCrAlY and CoCrAlY bond coatings was in general relatively short as compared with that with plasma-deposited bond coatings. With thin (0.003 to 0.006 cm) NiCrAlY and CoCrAlY coatings plasma deposited at the baseline conditions of 11 kW with argon over the sputtered bond coatings, the lives of the TBC were increased by more than 500 percent, but they were still significantly less than those with the more oxidation resistant, 0.015-cm-thick bond coatings that were deposited at 20 kW with the argon - 3.5-vol% H_2 arc gas. This is attributed to lower surface roughness and/or poor oxidation resistance of the added coating.

9. Cracking of the TBC on the rectangular specimens with the plasma-deposited bond coatings seemed to originate from microcracks within the TBC that formed at the corners of the specimens.

REFERENCES

1. Cavanagh, J. R.; et al.: The Graded Thermal Barrier - A New Approach for Turbine Engine Cooling. AIAA Paper 72-361, Apr. 1972.

2. Dapkunas, S. J.; and Clarke, R. L.: Evaluation of the Hot-Corrosion Behavior of Thermal Barrier Coatings - Sodium Compounds. NSRDC-4428, Naval Ship Research and Development Center, 1974.

3. Liebert, C. H.; and Stepka, F. S.: Potential Use of Ceramic Coating as a Thermal Insulation on Cooled Turbine Hardware. NASA TM X-3352, 1976.

4. Liebert, C. H.; et al.: Durability of Zirconia Thermal-Barrier Ceramic Coatings on Air-cooled Turbine Blades in Cyclic Jet Engine Operation. NASA TM X-3410, 1976.

5. Stecura, S.: Two Layer Thermal Barrier Coating for Turbine Airfoils - Furnace and Burner Rig Test Results. NASA TM X-3425, 1976.

6. Grisaffe, S. J.; and Levine, S. R.: Review of NASA Thermal Barrier Coating Programs for Aircraft Engines. Proceedings of the First Conference on Advanced Materials for Alternative Fuel Capable Directly Fired Heat Engines, CONF-790749, 1979, pp. 680-703.

7. Stecura, S.: Effects of Compositional Changes on the Performance of a Thermal Barrier Coating System. NASA TM-78976, 1978.

8. Stecura, S.: Effects of Yttrium, Aluminum, and Chromium Concentrations in Bond Coatings on the Performance of Zirconia-Yttria Thermal Barriers. NASA TM-79206, 1979.

9. Fairbanks, J. W.; Levine, S. R.; and Cohn, A.: Ceramic Coating Program Overview. Proceedings of the First Conference on Advanced Materials for Alternative Fuel Capable Directly Fired Heat Engines, CONF-790749, 1979, pp. 527-541.

10. Hodge, P. E.; et al.: Thermal Barrier Coatings: Rig Hot Corrosion Test Results. DOE/NASA/2593-78/3, NASA TM-79005, 1978.

11. Miller, R. A.: Analysis of the Response of a Thermal Barrier Coating to Sodium- and Vanadium-Doped Combustion Gases. DOE/NASA-2593-79/7, NASA TM-79205, 1979.

12. Hodge, P. E.; Miller, R. A.; and Gedwill, M. A.: Evaluation of Hot Corrosion Behavior of Thermal Barrier Coatings. DOE/NASA/2593-16, NASA TM-81520, 1980.

13. Barrett, C. A.; Santoro, G. J.; and Lowell, C. E.: Isothermal and Cyclic Oxidation at 1000° and 1100° C of Four Nickel-Base Alloys: NASA-TRW VIA B-1900, 713C, and 738X. NASA TN D-7484, 1973.

14. Barrett, C. A.; and Lowell, C. E.: Resistance of Nickel-Chromium-Aluminum Alloys to Cyclic Oxidation at 1100° and 1200° C. NASA TN D-8255, 1976.

15. Santoro, G. J.; and Barrett, C. A.: Hot Corrosion Resistance of Nickel-Chromium-Aluminum Alloys. J. Electrochem. Soc., vol. 125, no. 2, Feb. 1978, pp. 271-278.

16. Kahn, A. S.; Lowell, C. E.; and Barrett, C. A.: The Effect of Zirconium on the Isothermal Oxidation of Nominal Ni-14Cr-24Al Alloys. J. Electrochem. Soc., vol. 127, no. 3, Mar. 1980, pp. 670-679.

17. Barrett, C. A.; and Lowell, C. E.: Comparison of Isothermal and Cyclic Oxidation Behavior of Twenty-Five Commercial Sheet Alloys at 1150° C. Oxid. Met., vol. 9, no. 4, Aug. 1975, pp. 307-355.

18. Barrett, C. A.; and Lowell, C. E.: Resistance of Ni-Cr-Al Alloys to Cyclic Oxidation at 1100° and 1200° C. Oxid. Met., vol. 11, no. 4, Aug. 1977, pp. 199-223.

19. Barrett, C. A.; and Lowell, C. E.: The Cyclic Oxidation Resistance of Cobalt-Chromium-Aluminum Alloys at 1100° and 1200° C and Comparison with Nickel-Chromium-Aluminum Alloy System. Oxid. Met., vol. 12, no. 4, Aug. 1978, pp. 293-311.

20. Levine, S. R.: Adhesive/Cohesive Strength of a ZrO_2-12 w/o Y_2O_3/NiCrAlY Thermal Barrier Coating. NASA TM-73792, 1978.

21. Taylor, A.; and Floyd, R. W.: The Constitution of Nickel-Rich Alloys of the Nickel-Chromium-Aluminum System. J. Inst. Met., vol. 81, pt. 9, May 1953, pp. 451-464.

22. Tucker, R. C.; Taylor, T. A.; and Weatherly, M. H.: Plasma Deposited MCrAlY Airfoil and Zirconia/MCrAlY Thermal Barrier Coatings. Presented at the Third Conference on Gas Turbine Materials in a Marine Environment, Bath Univ., Bath, England, Sept. 20-23, 1976, Session VII, Paper 2.

23. Powder Diffraction File, Inorganic Compounds. Joint Committee on Powder Diffraction Standards, 1978.

TABLE I. - CHEMICAL ANALYSES OF PLASMA SPRAY POWDERS AND SUPERALLOY SUBSTRATES

Element	Thermal barrier oxide	Bond coatings			Substrates	
		NiCrAlY[a]	NiCrAlZr	CoCrAlY	B-1900 + Hf	MAR-M-509
	Content, wt%					
Al	0.06	5.56-14.36[b]	13.41	9.06	6.12	(c)
B	(c)	.018	(c)	.003	.013	0.006
C	(c)	.023	.007	.011	.11	.63
Ca	.24	<.001	<.001	<.001	(c)	(c)
Co	(c)	.075	.038	(d)	10.08	(d)
Cr	(c)	14.31-30.86[b]	14.06	19.96	8.17	23.63
Cu	(c)	.008	.025	.008	(c)	<.10
Fe	.16	.079	.048	.025	.19	.38
Hf	2.00	<.01	<.01	<.01	1.20	(c)
Mg	.06	<.001	<.001	<.001	(c)	(c)
Mn	(c)	.041	<.001	.003	.10	.10
Mo	↓	.005	<.005	<.005	6.10	(c)
Nb	↓	.018	<.01	<.01	.063	(c)
Ni	↓	(d)	(d)	.21	(d)	10.80
O_2	↓	.089	.026	.038	(c)	(c)
P	↓	.008	.002	.003	.015	.02
S	↓	.004	<.001	.001	.008	.009
Si	.23	.074	.066	.065	.10	.19
Ta	(c)	<.05	<.05	<.05	4.36	3.76
Ti	.06	.011	.008	<.005	.98	.25
V	(c)	.055	.008	.005	(c)	(c)
W	.01	.01	<.01	<.01	.05	7.35
Y	9.11	.11-.61[b]	<.01	.63	(c)	(c)
Zn	(c)	<.005	<.005	.005	(c)	(c)
Zr	(c)	.008	.10	.008	.05	.37

[a]Impurity values reported for the NiCrAlY powders are the maximum values encountered.

[b]Specific aluminum, chromium, and yttrium concentrations for each NiCrAlY powder are given in the text.

[c]Not determined.

[d]Major.

TABLE II. - PLASMA-DEPOSITION PARAMETERS FOR BOND COATINGS AND THERMAL BARRIER COATINGS

[Nozzle diameter of Plasmadyne SG-1B gun, 0.79 cm.]

Coatings	Arc gas	Parameters						
		Current, A	Voltage, V	Power, kw	Arc gas flow rate, m^3/hr	Powder carrier gas[a] flow rate, m^3/hr	Powder feed rate, g/min	Gun-to-specimen distance, cm
Bond coatings	Argon	350 450 550	31±2 31±2 31±2	11 14 17	1.54	0.34	13	13-15
	Argon - 3.5-vol% hydrogen	350 450 550	45±2 45±2 45±2	16 20 24				
Thermal barrier coatings	Argon	550	33±2	18	1.68	0.31	16	9-10

[a]Argon carrier gas.

TABLE III. - SUMMARY OF STATIC-AIR, CYCLIC FURNACE

Nominal bond coating thickness, cm	Plasma power, kW	Gas used in plasma deposition	Bond coating composition, wt%	Measured bond coating thickness,[b] cm	Final oxidation data	
					Specific weight change, mg/cm^2	Slope of oxidation, curve, mg/cm^2/hr
						1000° C/1200
0.010	11	Argon	Ni-16.2Cr-5.6Al-0.61Y	0.010, 0.011	+2.8	0
			Ni-18.0Cr-11.9Al-0.55Y	.010, .010	+2.7	+.001
			Ni-17.7Cr-12.2Al-0.11Y	.010, .010	+3.3	+.001
			Ni-30.9Cr-11.1Al-0.48Y	.011, .011	+4.0	+.001
			Ni-14.1Cr-13.4Al-0.10Zr	.011	+3.1	+.001
			Co-20.0Cr-9.1Al-0.63Y	.010, .011	-4.5	-.032
						1100° C/200
0.010	11	Argon	Ni-16.2Cr-5.6Al-0.61Y	0.012	-18.3	-0.410
			Ni-18.0Cr-11.9Al-0.55Y	.011, .010	-9.6	-.267
			Ni-15.8Cr-12.8Al-0.36Y	.010, .011	-6.6	-.015
			Ni-17.7Cr-12.2Al-0.11Y	.011	+4.7	+.027
			Ni-30.9Cr-11.1Al-0.48Y	.011, .011	+5.5	-.010
			Ni-14.1Cr-13.4Al-0.10Zr	.010, .011	+5.2	-.086
			Co-20.0Cr-9.1Al-0.63Y	.011, .009	-29.3	-.020
0.015			Ni-15.8Cr-12.8Al-0.36Y	0.015	+7.8	+0.047
			Ni-17.7Cr-12.2Al-0.11Y	.014	+5.4	+.011
0.010	14	Argon	Ni-18.0Cr-11.9Al-0.55Y	0.010	-7.7	-0.183
			Ni-15.8Cr-12.8Al-0.36Y	.009	-3.5	-.187
			Ni-30.9Cr-11.1Al-0.48Y	.010	+3.4	-.013
0.015			Ni-18.0Cr-11.9Al-0.55Y	0.014	+2.1	-0.026
			Ni-15.8Cr-12.8Al-0.36Y	.013	+3.9	+.007
			Ni-30.9Cr-11.1Al-0.48Y	.015	+4.3	+.012
			Ni-14.1Cr-13.4Al-0.10Zr	.016	+2.9	+.012
0.010	17	Argon	Ni-15.8Cr-12.8Al-0.36Y	0.009, 0.010	-3.3	-0.102
0.015			Ni-15.8Cr-12.8Al-0.36Y	0.014, 0.015	+3.1	+0.009
0.010	16	Argon - 3.5-vol% H_2	Ni-15.8Cr-12.8Al-0.36Y	0.010, 0.009	-5.7	-0.143
0.015			Ni-15.8Cr-12.8Al-0.36Y	0.014	+2.8	+0.005
			Ni-14.1Cr-13.4Al-0.10Zr	.015	+2.9	+.004
0.010	20	Argon - 3.5-vol% H_2	Ni-18.0Cr-11.9Al-0.55Y	0.010	-7.0	-0.123
			Ni-15.8Cr-12.8Al-0.36Y	.009	+1.4	-.033
			Ni-30.9Cr-11.1Al-0.48Y	.010	+2.6	+.009
			Ni-14.1Cr-13.4Al-0.10Zr	.010	+2.5	+.003
0.015			Ni-18.0Cr-11.9Al-0.55Y	0.014, 0.014	-0.3	-0.021
			Ni-15.8Cr-12.8Al-0.36Y	.015	+2.7	+.003
			Ni-17.7Cr-12.2Al-0.11Y	.015	+2.7	+.002
			Ni-30.9Cr11.1Al-0.48Y	0.014, 0.013	+2.7	+0.002
			Ni-14.3Cr-14.4Al0.16Y	.015, .014	+2.9	+.007
			Ni-14.1Cr-13.4Al-0.10Zr	.015	+3.4	+.005
0.015	24	Argon - 3.5-vol% H_2	Ni-15.8Cr-12.8Al-0.36Y	0.014	+3.3	+0.003

[a]Cycles: 1 hr at test temperature and 20-min or more cooling.
[b]Measured with a vernier caliper. Values listed are average maximums for the major surfaces. In some instances duplicate specimens were tested.
[c]Relative pattern intensities: Major phases - vs, very strong; s, strong; m, medium. Minor phases - w, weak; vw, very weak; t, trace.
[d]Estimated lattice spacing a_0 of spinel in nanometers (±0.05 nm); values reported in ref. 23: $NiAl_2O_4$, 0.805; $NiCr_2O_4$, 0.832; $CoAl_2O_4$, 0.810; $CoCr_2O_4$, 0.832.
[e]Not determined because bond coating heavily oxidized and spalled.

OXIDATION[a] RESULTS FOR BOND COATINGS ON B-1900 + Hf

X-ray diffraction analyses of retained oxide scales	
Major phases (relative intensities)[c]	Minor phases (relative intensities)[c]
-hr oxidation	
Alloy (s), Cr_2O_3 (m) Alloy (s), NiO (m) Alloy (s), α-Al_2O_3 (s), spinel (s) 0.805 Alloy (vs), α-Al_2O_3 (m) Alloy (vs), α-Al_2O_3 (s), spinel (s) 0.805 (e)	Spinel (w) 0.820[d] Spinel (w) 0.805, spinel (w) 0.825, α-Al_2O_3 (w) Cr_2O_3 (vw) Spinel (vw) 0.820, spinel (t) 0.805, Cr_2O_3 (t) --- (e)
-hr oxidation	
(e) (e) (e) Alloy (s), spinel (s) 0.810, α-Al_2O_3 (m) Alloy (s), spinel (s) 0.810, α-Al_2O_3 (m) Alloy (vs), spinel (s) 0.810, NiO (s), α-Al_2O_3 (m) (e)	(e) (e) (e) NiO (w), spinel (w) 0.825 --- Spinel (w) 0.825, ZrO_2 or HfO_2 (vw)
Alloy (vs), α-Al_2O_3 (vs), spinel (m) 0.820 Alloy (s), α-Al_2O_3 (s), spinel (m) 0.810	Cr_2O_3 (t) Cr_2O_3 (w), NiO (w)
(e) (e) Alloy (vs), spinel (s) 0.810, α-Al_2O_3 (m)	(e) (e) Cr_2O_3 (w)
Alloy (s), spinel (s) 0.810, α-Al_2O_3 (m) α-Al_2O_3 (vs), spinel (s) 0.815, alloy (s) Alloy (vs), α-Al_2O_3 (m) Alloy (s), α-Al_2O_3 (s), spinel (s) 0.805	NiO (w), Cr_2O_3 (w), spinel (vw), 0.825, HfO_2 (vw) Rutile (vw), HfO_2 (vw), Cr_2O_3 (t) Spinel (w) 0.810 Cr_2O_3 (t) NiO (w), Cr_2O_3 (w)
(e)	(e)
Alloy (s), α-Al_2O_3 (s), spinel (s) 0.805	Cr_2O_3 (vw), HfO_2 (vw)
(e)	(e)
Alloy (vs), α-Al_2O_3 (s) Alloy (s), α-Al_2O_3 (s), spinel (s) 0.805	Spinel (t) 0.805, Cr_2O_3 (t) NiO (vw), ZrO_2 or HfO_2 (vw)
(e) Alloy (s), α-Al_2O_3 (s), spinel (s) 0.805 Alloy (vs), α-Al_2O_3 (s) Alloy (s), α-Al_2O_3 (s), spinel (s) 0.805	(e) Cr_2O_3 (w) Rutile/TRI-rutile (vw), HfO_2 (vw) Spinel (w) 0.815, Cr_2O_3 (vw) Rutile/TRI-rutile (vw), ZrO_2 or HfO_2 (vw)
Alloy (s), α-Al_2O_3 (s), spinel (s) 0.805, NiO (m) Alloy (vs), α-Al_2O_3 (vs) Alloy (s), α-Al_2O_3 (s), spinel (m) 0.805 Alloy (s), α-Al_2O_3 (s), spinel (s) 0.810 Alloy (s), α-Al_2O_3 (s), spinel (m) 0.805 Alloy (s), α-Al_2O_3 (s), spinel (s) 0.805	--- Spinel (t) 0.805, Cr_2O_3 (t) HfO_2 (vw) --- HfO_2 (vw) ZrO_2 or HfO_2 (vw)
Alloy (s), α-Al_2O_3 (s), spinel (m) 0.805	$3Y_2O_3.5Al_2O_3$ (vw)

TABLE IV. - SUMMARY OF STATIC-AIR, CYCLIC FURNACE

Nominal bond coating thickness, cm	Plasma power, kW	Gas used in plasma deposition	Bond coating composition, wt%	Measured bond coating thickness,[b] cm	Final oxidation data	
					Specific weight change, mg/cm^2	Slope of oxidation, curve, mg/cm^2/hr
						1000° C/1200
0.010	11	Argon	Ni-16.2Cr-5.6Al-0.61Y	0.011	+4.6	+0.002
			Ni-18.0Cr-11.9Al-0.55Y	.011, .011	+4.9	+.001
			Ni-30.9Cr-11.1Al-0.48Y	.009	+2.8	.000
			Co-20.0Cr-9.1Al-0.63Y	.010	+6.2	+.002
						1100° C/200
0.010	11	Argon	Ni-16.2Cr-5.6Al-0.61Y	0.011, 0.011	-47.7	-0.537
			Ni-18.0Cr-11.9Al-0.55Y	.012	-17.9	-.540
			Ni-15.0Cr-12.8Al-0.30Y	.010, .010	+4.9	-.007
			Ni-30.9Cr-11.1Al-0.48Y	.010, .010	-18.2	-.639
			Ni-14.1Cr-13.4Al-0.10Zr	.010, .009	-9.1	-.292
			Co-20.0Cr-9.1Al-0.63Y	.011, .011	-52.0	-1.443
0.010	14	Argon	Ni-30.9Cr-11.1Al-0.48Y	0.010	+3.7	-0.020
0.015			Ni-30.9Cr-11.1Al-0.48Y	0.015	+5.1	+0.012
0.010	16	Argon - 3.5-vol% H_2	Ni-15.0Cr-12.8Al-0.36Y	0.010, 0.010	+4.5	+0.010
			Ni-14.5Cr-13.4Al-0.10Zr	.010, .009	-1.6	-.420
0.015	20	Argon - 3.5-vol% H_2	Ni-15.0Cr-12.8Al-0.36Y	0.014, 0.014	+5.0	+0.013
			Ni-30.9Cr-11.1Al-0.48Y	.015, .016	+4.4	+.010
0.015	24	Argon - 3.5-vol% H_2	Ni-30.9Cr-11.1Al-0.48Y	0.015	+5.3	+0.013

[a]Cycles: 1 hr at test temperature and 20-min or more cooling.
[b]Measured with a vernier caliper. Values listed are average maximums for the major surfaces. In some instances duplicate specimens were tested.
[c]Relative pattern intensities: Major phases - vs, very strong; s, strong; m, medium. Minor phases - w, weak; vw, very weak; t, trace.
[d]Estimated lattice spacing a_0 of spinel in nanometers (±0.05 nm); values reported in ref. 23: $NiAl_2O_4$, 0.805; $NiCr_2O_4$, 0.832; $CoAl_2O_4$, 0.810; $CoCr_2O_4$, 0.832.
[e]Not determined because bond coating heavily oxidized and spalled.

OXIDATION[a] RESULTS FOR BOND COATINGS ON MAR-M-509

X-ray diffraction analyses of retained oxide scales	
Major phases (relative intensities)[c]	Minor phases (relative intensities)[c]
-hr oxidation	
Spinel (s) 8.25[d], alloy (m) Alloy (s), NiO (m) Alloy (s), Cr_2O_3 (m) Spinel (s) 0.830	Cr_2O_3 (vw) α-Al_2O_3 (vw), Cr_2O_3 (vw), spinel (vw) 0.825, spinel (vw) 0.815 Spinel (vw) 0.825, α-Al_2O_3 (t) Spinel (t) 0.825
-hr oxidation	
(e) (e) Alloy (s), spinel (s) 0.810, α-Al_2O_3 (m), Cr_2O_3 (m) (e) (e) (e)	(e) (e) Spinel (w) 0.825 (e) (e) (e)
Spinel (s) 0.815, alloy (m)	Cr_2O_3 (w), α-Al_2O_3 (w)
Alloy (s), α-Al_2O_3, spinel (s) 0.810, Cr_2O_3 (m)	----------
Alloy (s), spinel (s) 0.810, α-Al_2O_3 (m) (e)	Cr_2O_3 (w), spinel (w) 0.825, rutile/trirutile (w) (e)
Alloy (s), α-Al_2O_3 (s), spinel (s) 0.810 Alloy (s), α-Al_2O_3 (s), spinel (s) 0.810	Cr_2O_3 (vw) Cr_2O_3 (vw)
Alloy (s), α-Al_2O_3 (s), spinel (s) 0.810	Cr_2O_3 (w), $3Y_2O_3.Al_2O_3$ (vw)

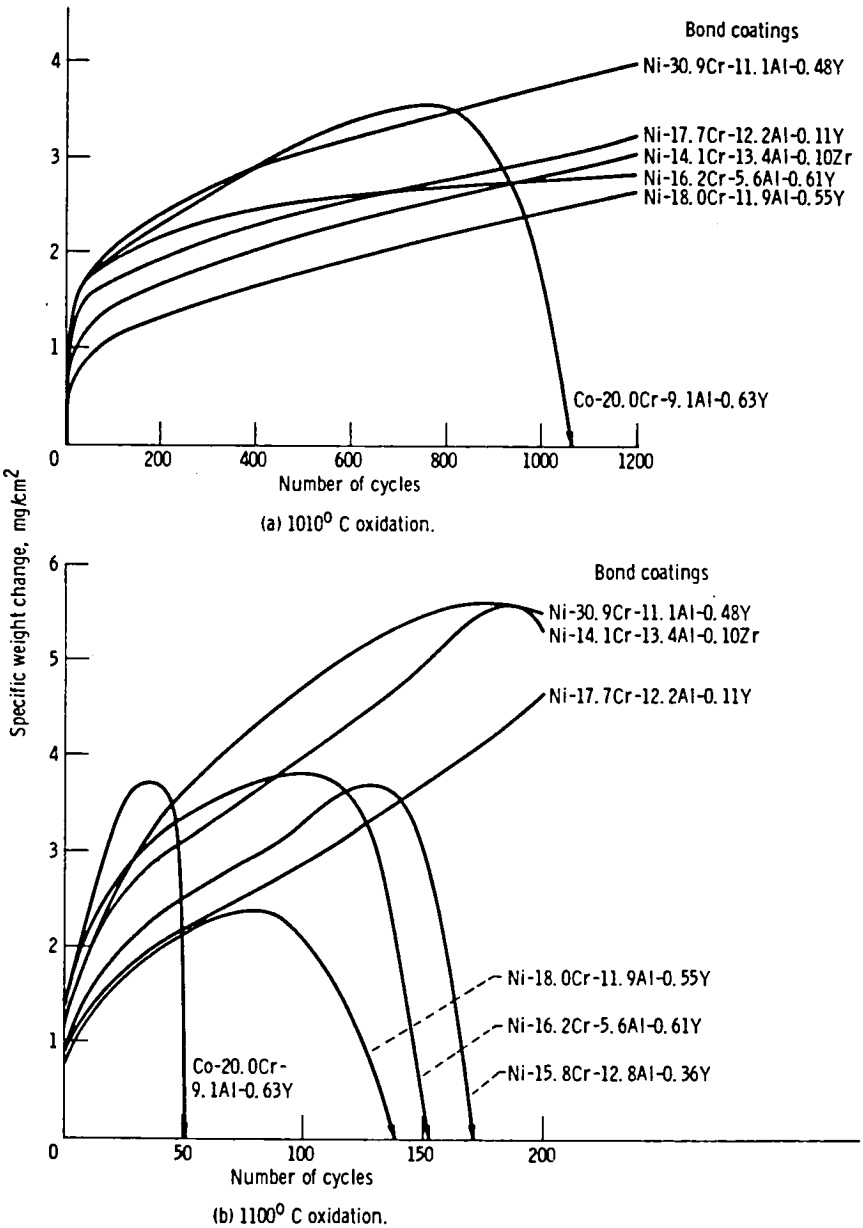

Figure 1. - Effect of oxidation temperature on weight-change behavior of 0.010-cm-thick plasma-deposited bond coatings on B-1900 + Hf in cyclic furnace oxidation at 1000° and 1100° C in static air. Cycles: 1 hr at test temperature and 20 min or more cooling. Coatings applied at 11 kW with argon arc gas.

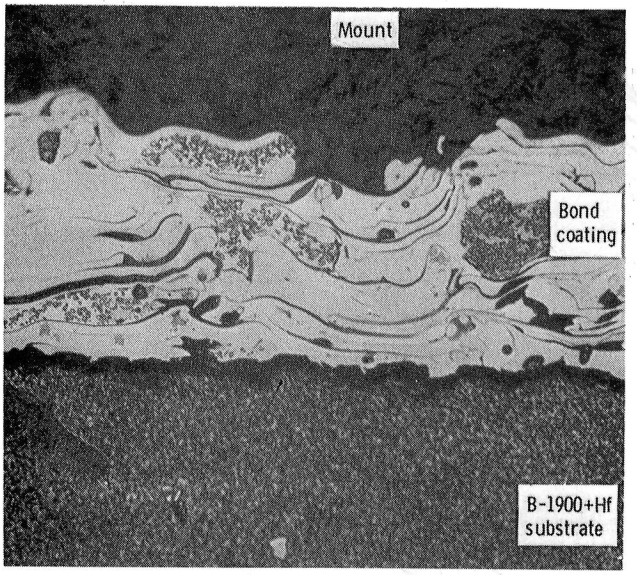

(a) As coated.

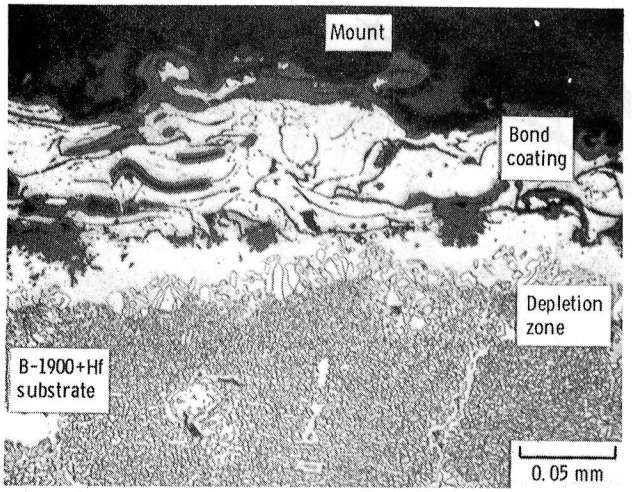

(b) After oxidation for 1200 hr at 1000^{0} C (1-hr cycles) in static air.

Figure 2. - Photomicrographs of plasma-deposited Ni-17.7Cr-12.2Al-0.11Y coating on B-1900+Hf. Coatings applied at 11 kW with argon arc gas. Nominal coating thickness, 0.010 cm.

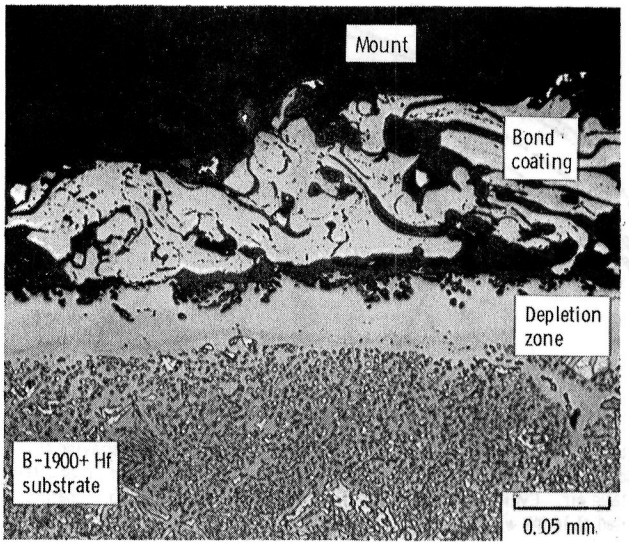

(c) After oxidation for 200 hr at 1100° C (1-hr cycles) in static air.

Figure 2. - Concluded.

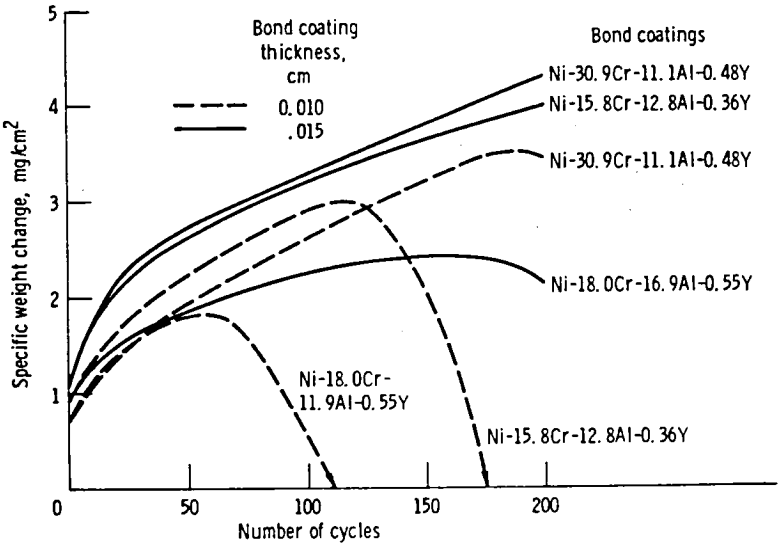

Figure 3. - Effect of bond coating thickness on weight-change behavior of plasma-deposited bond coatings on B-1900 + Hf in cyclic furnace oxidation at 1100° C in static air. Cycles: 1 hr at 1100° C and 20 min or more cooling. Coatings applied at 14 kW with argon arc gas.

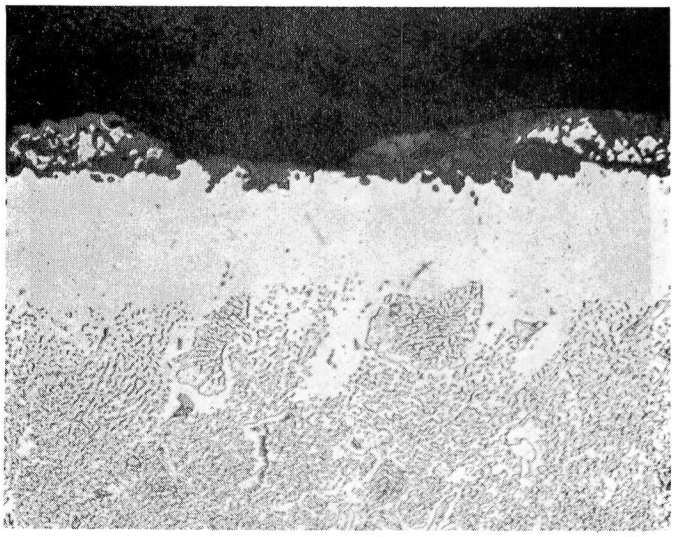

(a-1) Nominal coating thickness, 0.010 cm.

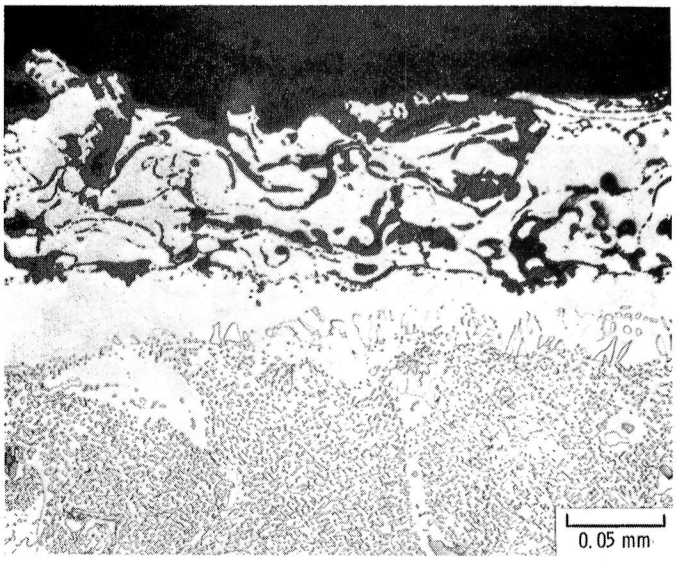

(a-2) Nominal coating thickness, 0.015 cm.

(a) Ni-15.8Cr-12.8Al-0.36Y bond coating.

Figure 4. - Photomicrographs of plasma-deposited Ni-15.8Cr-12.8Al-0.36Y and Ni-30.9Cr-11.1Al-0.48Y bond coatings on B-1900+Hf showing the effect of bond coating thickness after 200 hr of oxidation at 1100^{0} C in static air (1-hr cycles). Coatings applied at 14 kW with argon arc gas.

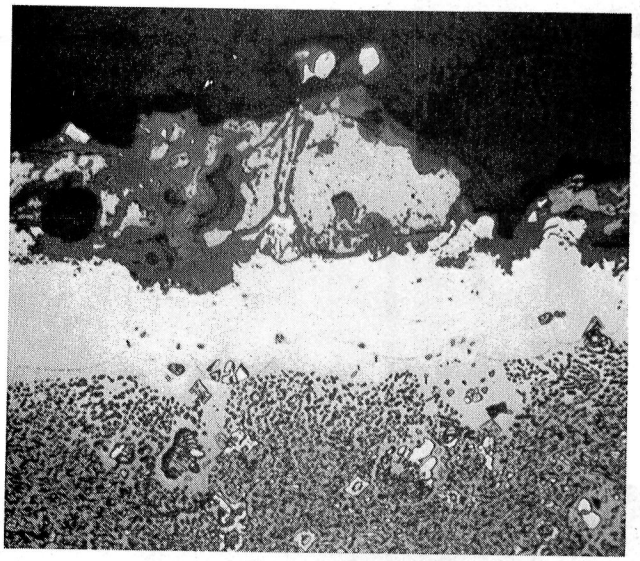

(b-1) Nominal coating thickness, 0.010 cm.

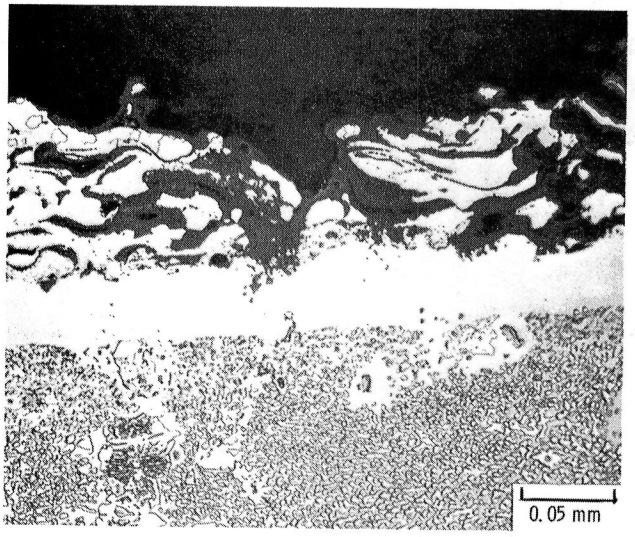

(b-2) Nominal coating thickness, 0.015 cm.

(b) Ni-30.9Cr-11.1Al-0.48Y bond coating.

Figure 4. - Concluded.

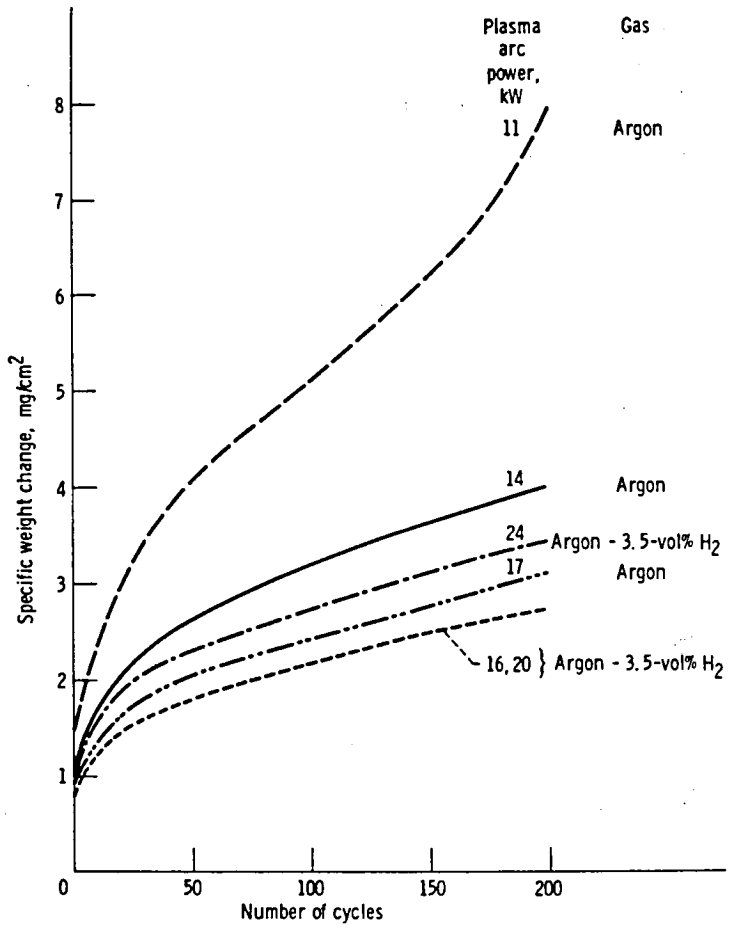

Figure 5. - Effect of plasma-deposition parameters on weight-change behavior of Ni-15.8Cr-12.8Al-0.36Y bond coating on B-1900 + Hf in cyclic furnace oxidation at 1100° C in static air. Nominal coating thickness, 0.015 cm.

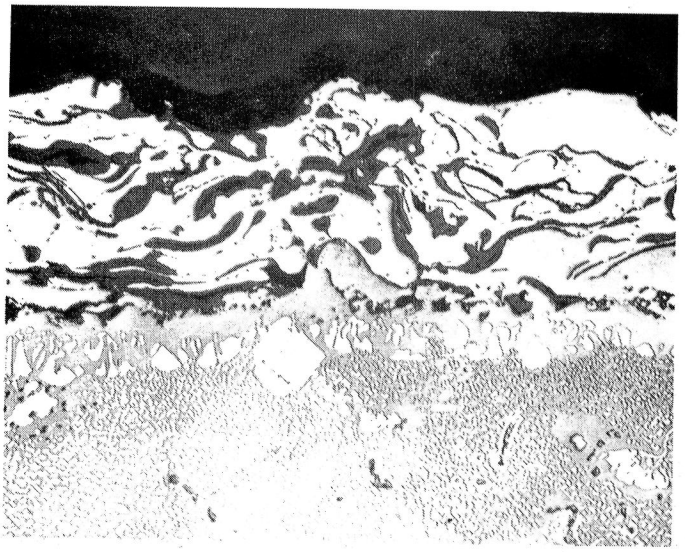

(a) Coating applied at 17 kW with argon arc gas.

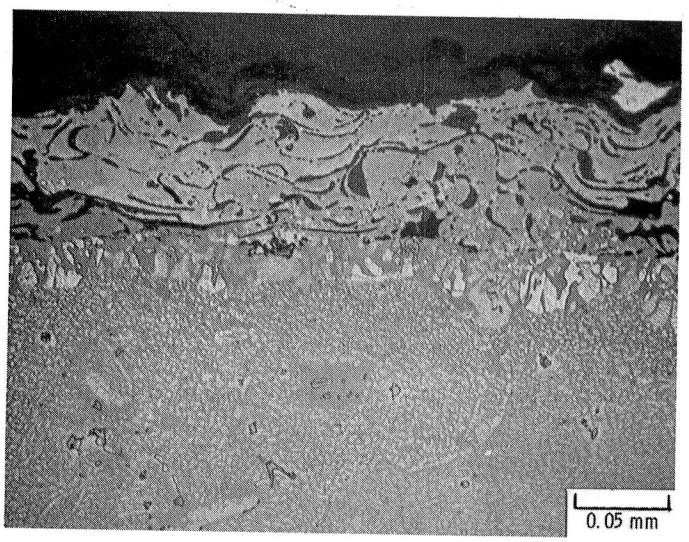

(b) Coating applied at 16 kW with argon - 3.5-vol% H_2 arc gas.

Figure 6. - Photomicrographs of plasma-deposited Ni-15.8Cr-12.8Al-0.36Y bond coatings on B-1900+Hf showing the effect of plasma-deposition parameters after 200 hr of oxidation at 1100° C in static air (1-hr cycles). Nominal coating thickness, 0.015 cm.

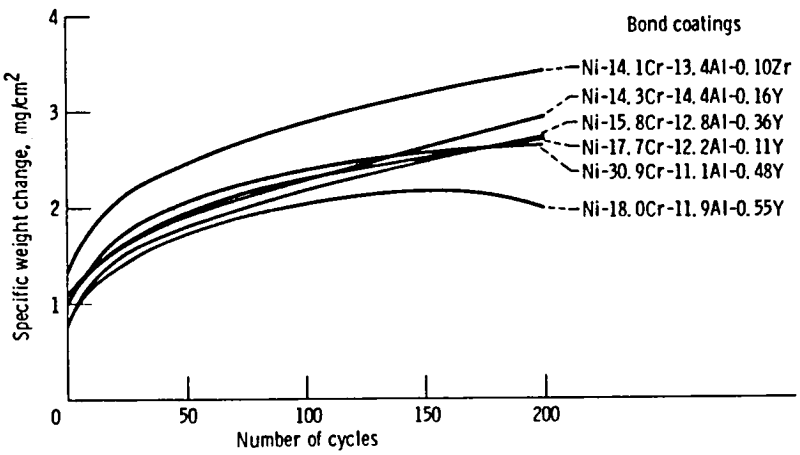

Figure 7. - Effect of optimized plasma-deposition parameters on weight-change behavior of various bond coatings on B-1900 + Hf in cyclic furnace oxidation at 1100° C in static air. Coatings applied at 20 kW with argon - 3.5-vol% H_2 arc gas. Nominal coating thickness, 0.015 cm.

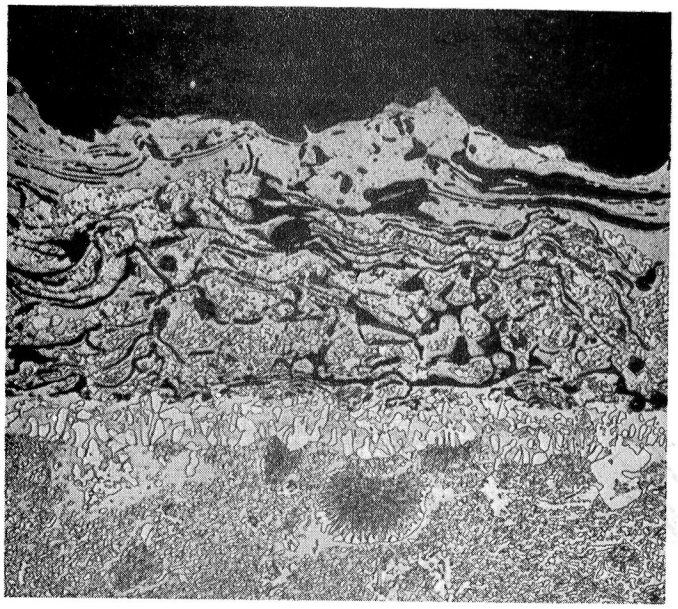

(a) Ni-14.3Cr-14.4Al-0.16Y bond coating.

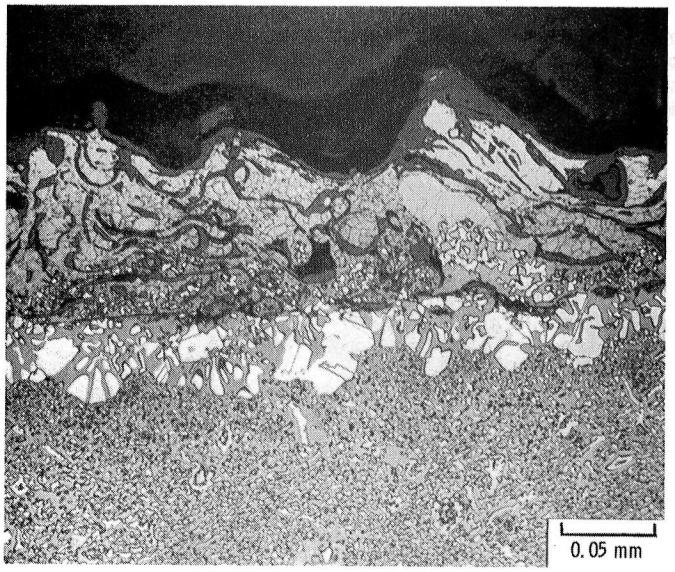

(b) Ni-14.1Cr-13.4Al-0.10Zr bond coating.

Figure 8. - Photomicrographs of plasma-deposited bond coatings on B-1900+Hf showing the effect of optimized deposition parameters after 200 hr of cyclic oxidation at 1100° C in static air (1-hr cycles). Coatings applied at 20 kW with argon - 3.5-vol% H_2 arc gas.

(c) Ni-15.8Cr-12.8Al-0.36Y bond coating.

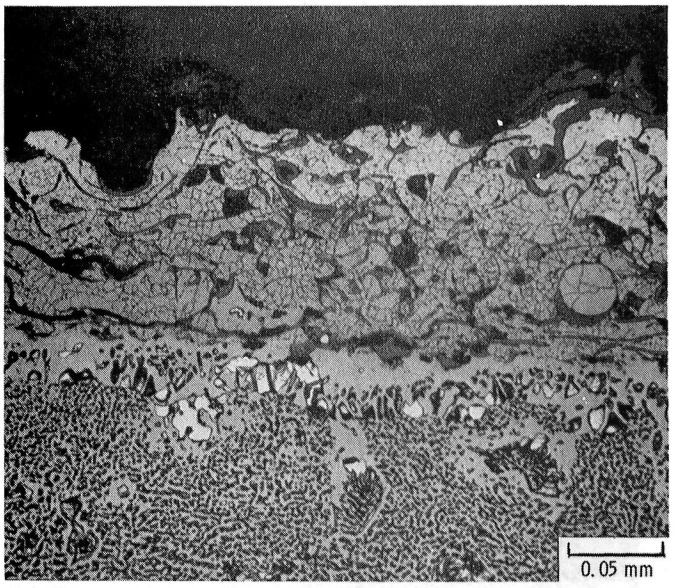

(d) Ni-17.7Cr-12.2Al-0.11Y bond coating.

Figure 8. - Continued.

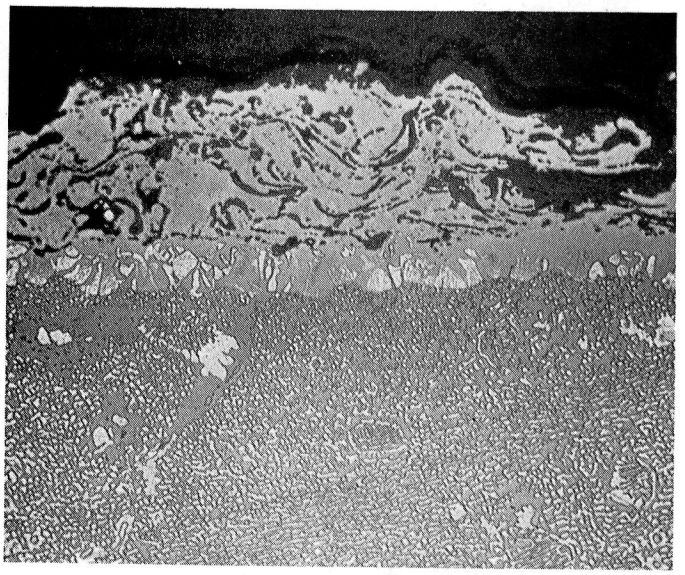

(e) Ni-18.0Cr-11.9Al-0.55Y bond coating.

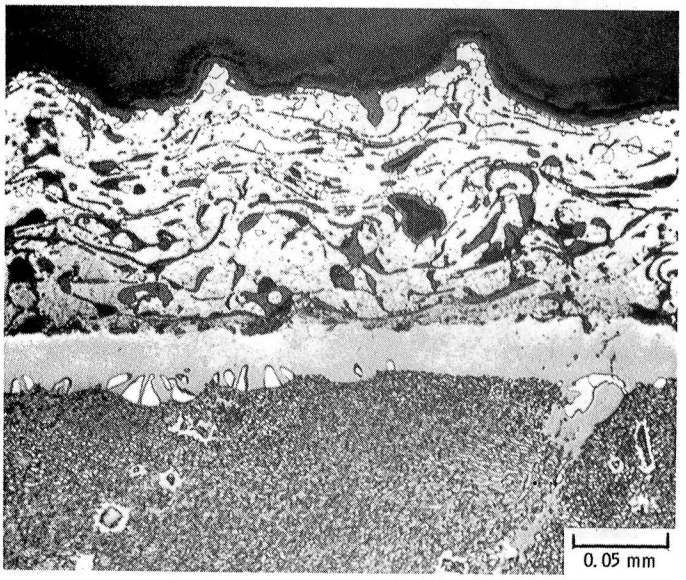

(f) Ni-30.9Cr-11.1Al-0.48Y bond coating

Figure 8. - Concluded.

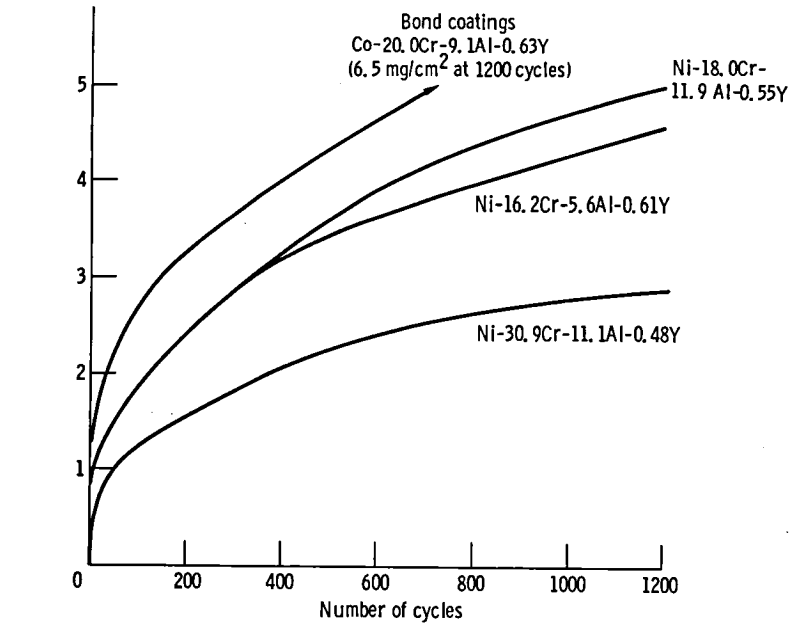

(a) 1000° C oxidation.

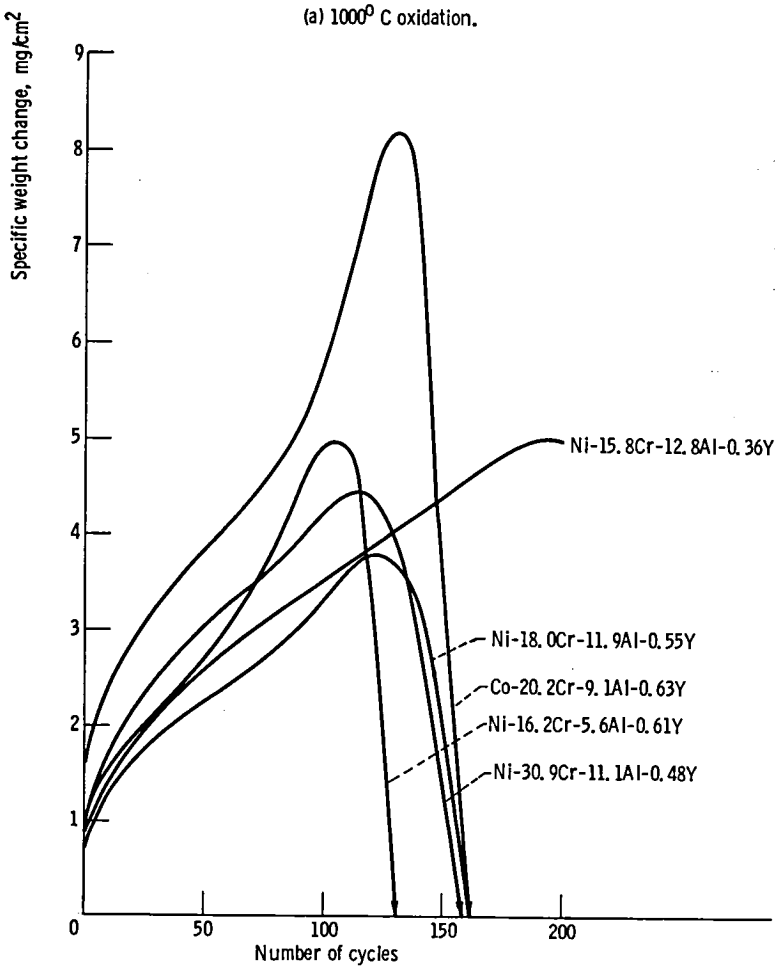

(b) 1100° C oxidation.

Figure 9. - Effect of oxidation temperature on weight-change behavior of 0.010-cm-thick plasma-deposited bond coatings on MAR-M-509 in cyclic furnace oxidation in static air. Cycles: 1 hr at test temperature and 20 min or more cooling. Coatings applied at 11 kW with argon arc gas.

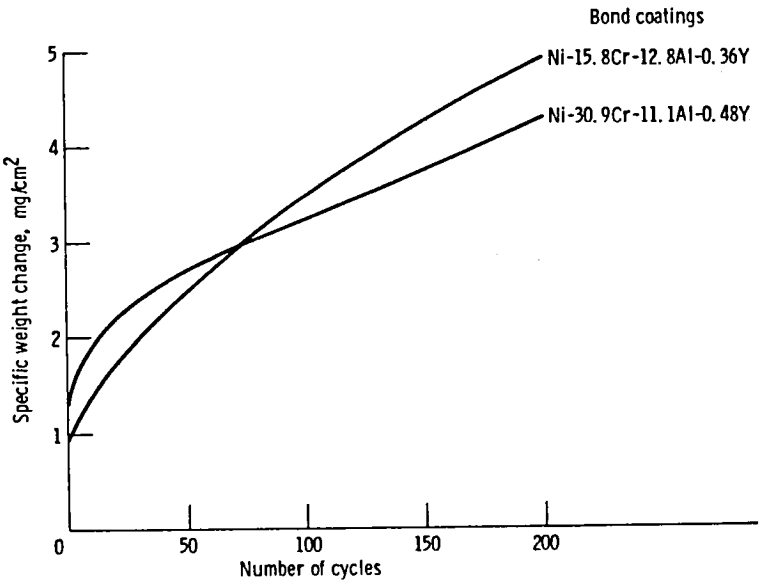

Figure 10. - Effect of optimized plasma-deposition parameters on weight-change behavior of Ni-15.8Cr-12.8Al-0.36Y and Ni-30.9Cr-11.1Al-0.48Y bond coatings on MAR-M-509 in cyclic furnace oxidation at 1100° C in static air. Coatings applied at 20 kW with argon - 3.5-vol% H_2 arc gas. Nominal coating thickness, 0.015 cm.

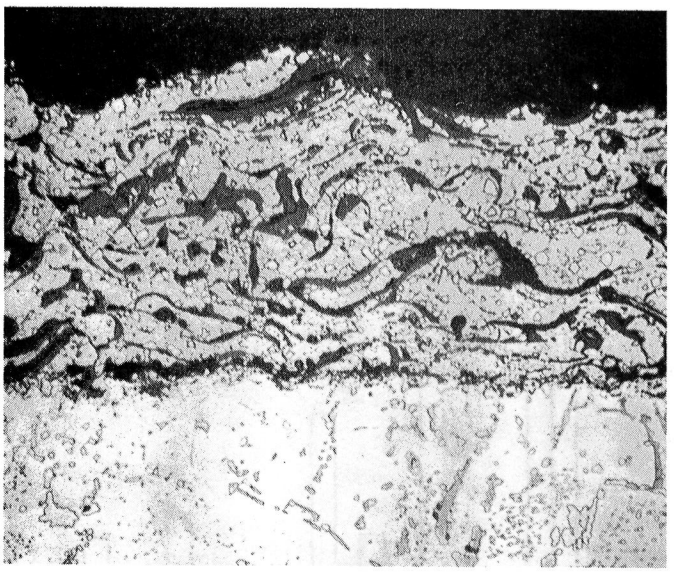

(a) Ni-30.9Cr-11.1Al-0.48Y bond coating.

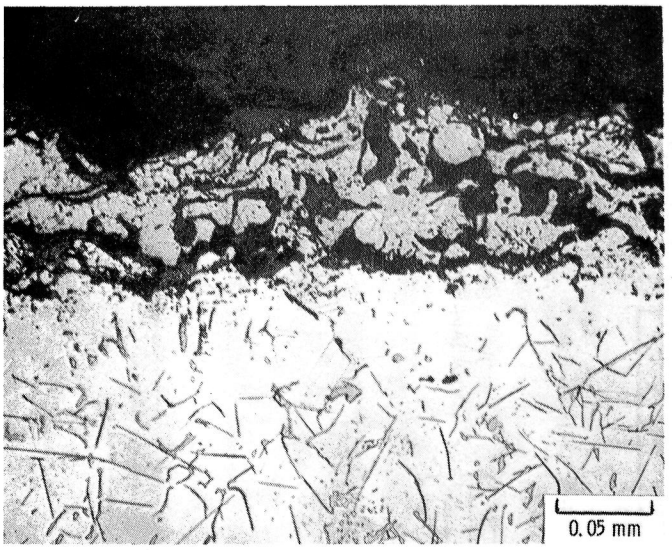

(b) Ni-15.8Cr-12.8Al-0.36Y bond coating.

Figure 11. - Photomicrographs of plasma-deposited bond coatings on MAR-M-509 showing the effect of optimized deposition parameters after 200 hr of oxidation at 1100° C in static air (1-hr cycles). Coatings applied at 20 kW with argon - 3.5-vol% H_2 arc gas. Nominal coating thickness, 0.015 cm.

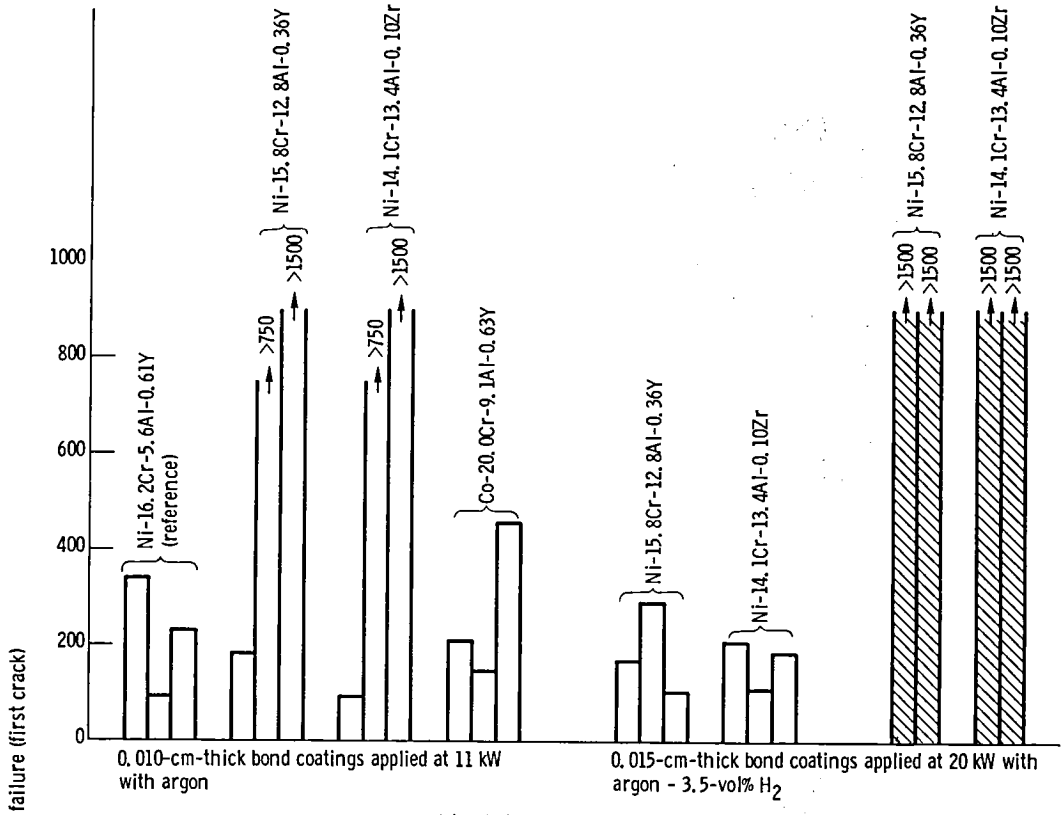

(a) B-1900 + Hf substrate.

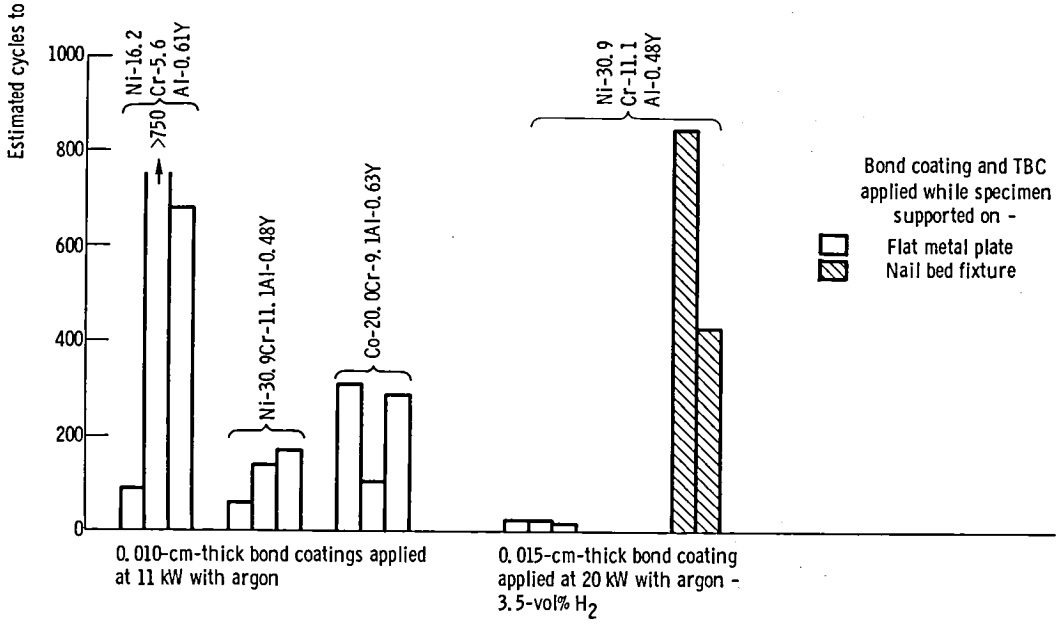

(b) MAR-M-509 substrate.

Figure 12. - Cyclic furnace endurance of ZrO_2-12Y_2O_3 thermal barrier coating with various plasma-deposited bond coatings on B-1900 + Hf and MAR-M-509 at 1010° C in static air. Cracking observed at ≤10X magnification. Nominal TBC thickness, 0.038 cm.

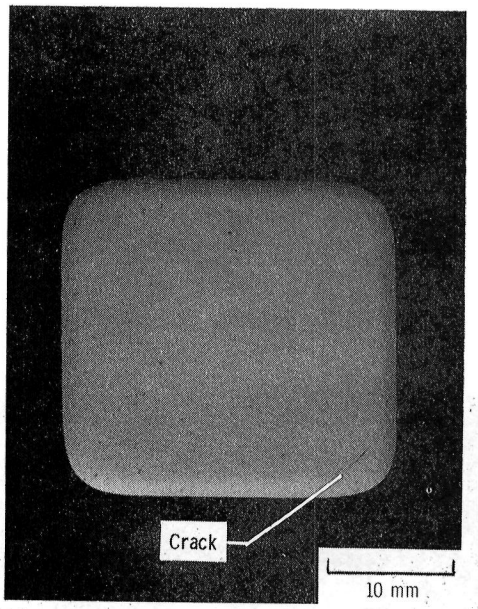

(a) Specimen showing a crack in TBC near lower right corner.

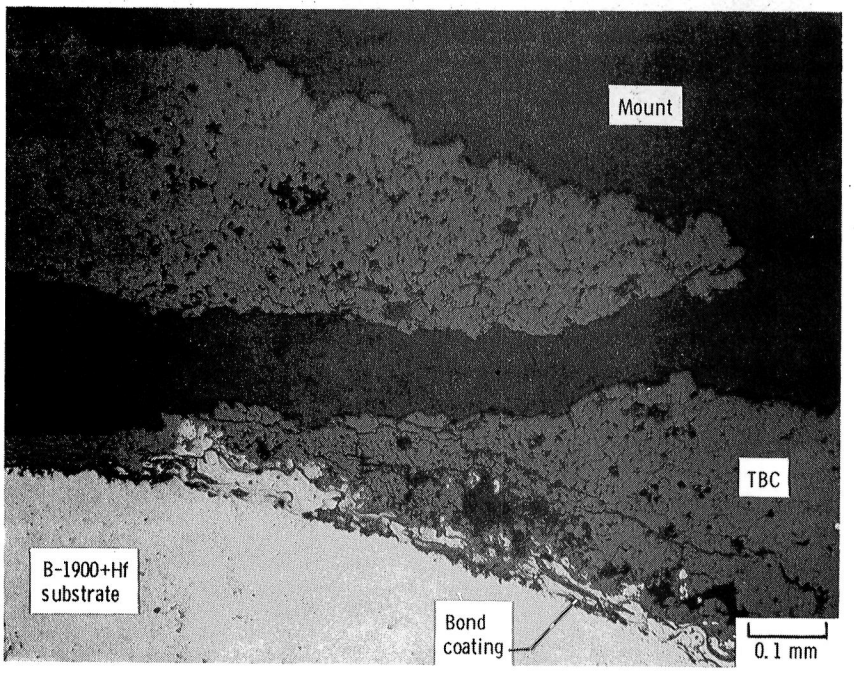

(b) Cross section of specimen shown in (a) above.

Figure 13. - Cracking of a thermal barrier coating on an endurance test specimen after 750 cycles at 1010° C. Crack was observed after about 337 cycles. ZrO_2-12Y_2O_3/Ni-16.2Cr-5.6Al-0.61Y (plasma-deposited) coated B-1900+Hf. Nominal coating thickness: TBC, 0.038 cm; bond coating, 0.010 cm. Bond coating applied at 11 kW with argon arc gas.

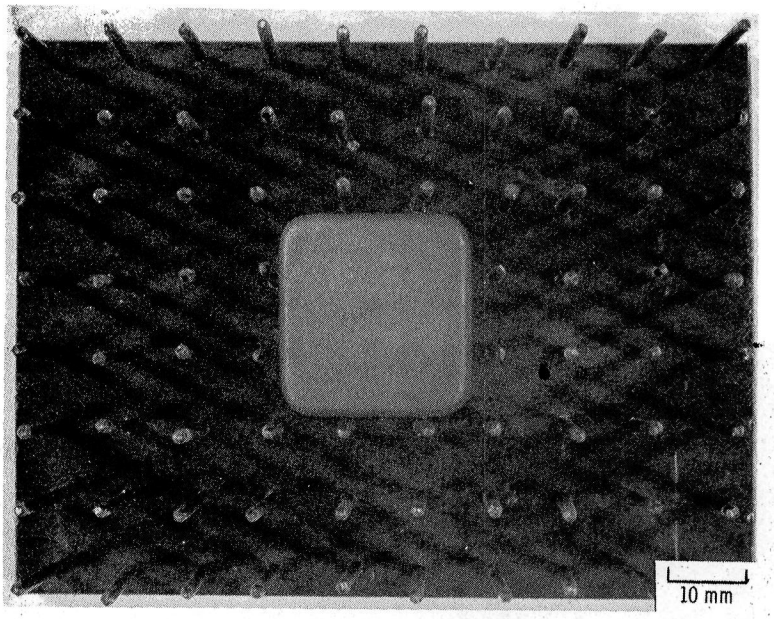

Figure 14. - Specimen on a nail bed fixture before coating by plasma deposition.

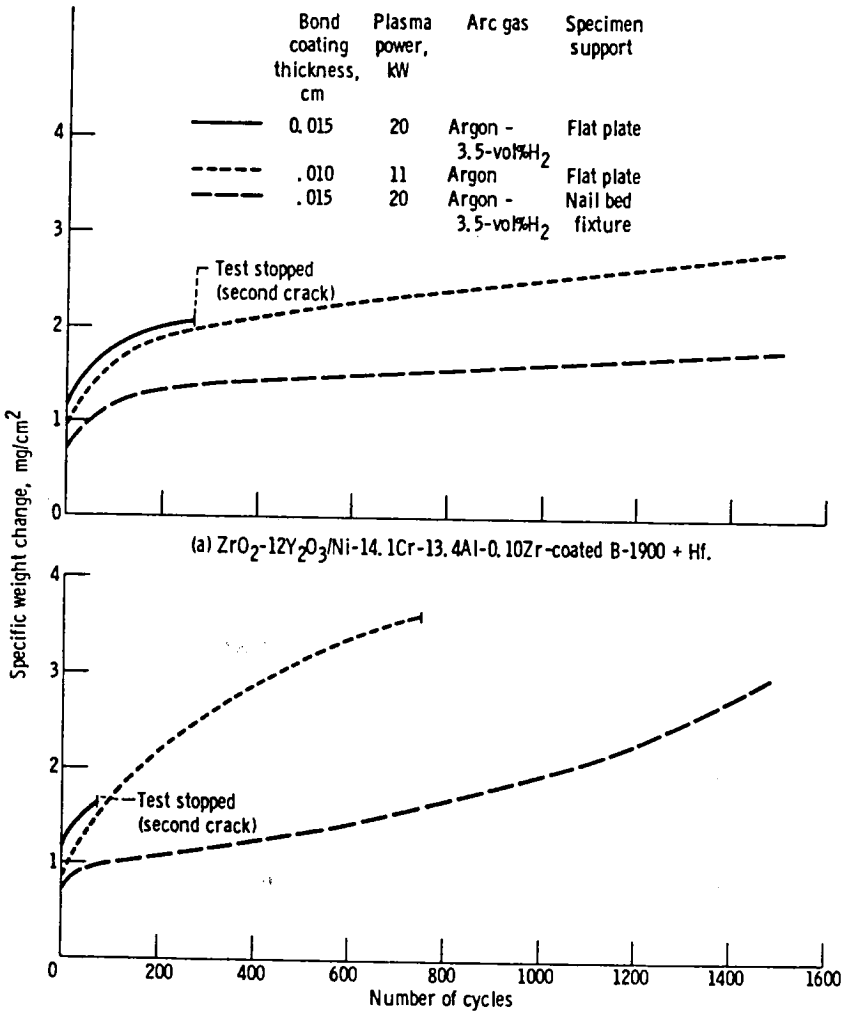

(a) ZrO_2-12Y_2O_3/Ni-14.1Cr-13.4Al-0.10Zr-coated B-1900 + Hf.

(b) ZrO_2-12Y_2O_3/Ni-30.9Cr-11.1Al-0.48Y-coated MAR-M-509.

Figure 15. - Weight change behavior of plasma-deposited thermal barrier coating plus bond coatings on B-1900 + Hf and MAR-M-509 in cyclic furnace endurance at 1010° C. Nominal TBC thickness, 0.038 cm.

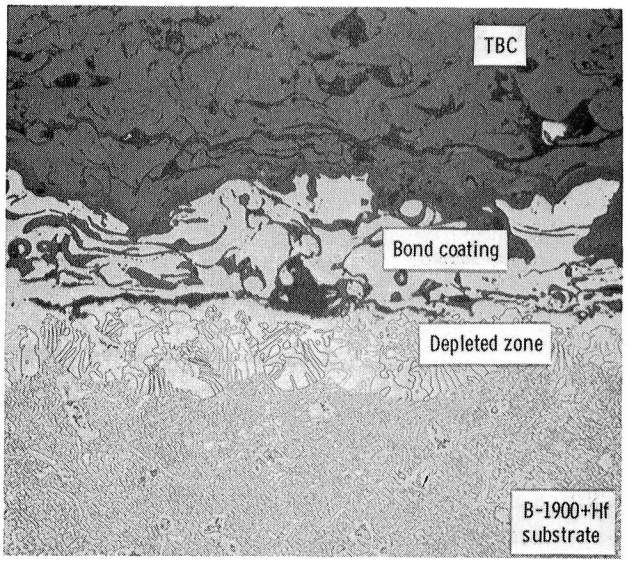

(a) 0.010-cm-thick bond coating applied at 11 kW with argon. Thermal barrier coating and bond coating applied on substrate supported on flat metal plate.

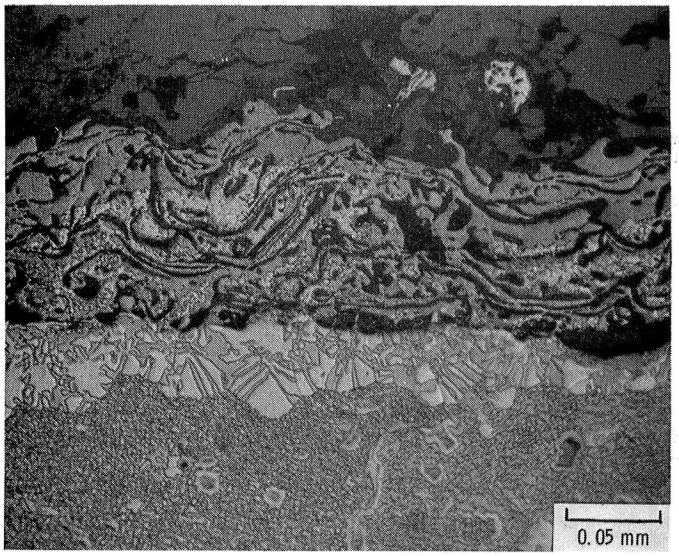

(b) 0.015-cm-thick bond coating applied at 20 kW with argon - 3.5-vol% H_2. Thermal barrier coating and bond coating applied on substrate supported on nail bed fixture.

Figure 16. - Photomicrographs of ZrO_2-12Y_2O_3/Ni-14.1Cr-13.4Al-0.10Zr coated B-1900+Hf after 1500 cycles of furnace endurance.

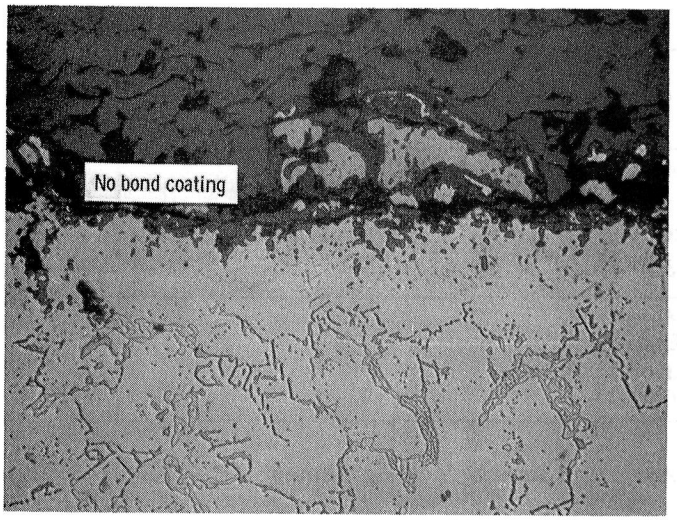

(a) 0.010-cm-thick bond coating applied at 11 kW with argon. Thermal barrier coating and bond coating applied on substrate supported on flat metal plate. After 750 cycles.

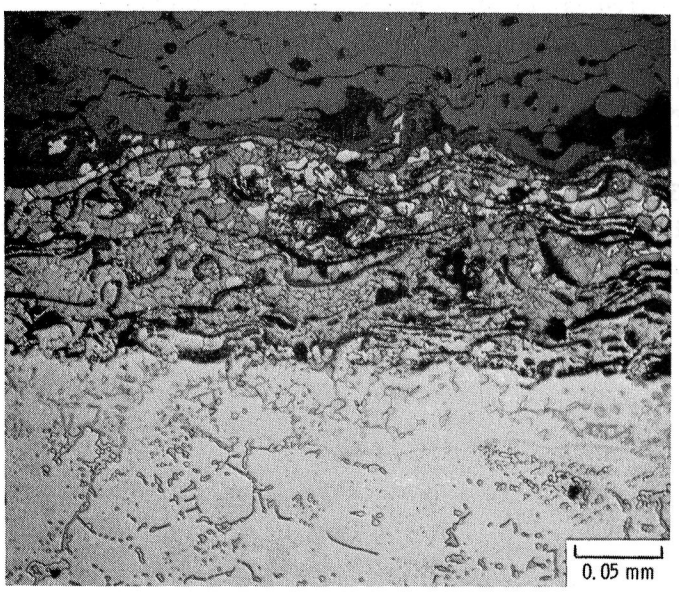

(b) 0.015-cm-thick bond coating applied at 20 kW with argon - 3.5-vol% H_2. Thermal barrier coating and bond coating applied on substrate supported on nail bed fixture. After 1500 cycles.

Figure 17. - Photomicrographs of ZrO_2-12Y_2O_3/Ni-30.9Cr-11.1Al-0.48Y coated MAR-M-509 after cyclic furnace endurance to 1010° C.

1. Report No.	2. Government Accession No.	3. Recipient's Catalog No.
NASA TM-81567		

4. Title and Subtitle	5. Report Date
IMPROVED BOND COATINGS FOR USE WITH THERMAL BARRIER COATINGS	September 1980
	6. Performing Organization Code
7. Author(s)	8. Performing Organization Report No.
Michael A. Gedwill	E-532
	10. Work Unit No.
9. Performing Organization Name and Address National Aeronautics and Space Administration Lewis Research Center Cleveland, Ohio 44135	11. Contract or Grant No.
	13. Type of Report and Period Covered Technical Memorandum
12. Sponsoring Agency Name and Address U.S. Department of Energy Office of Coal Utilization Washington, D.C. 20545	14. Sponsoring Agency ~~Code~~ Report No. DOE/NASA/2593-18

15. Supplementary Notes

Final report. Prepared under Interagency Agreement EF-77-A-01-2593.

16. Abstract

The potential for improving the durability of thermal barrier coatings (TBC's) being developed for coal-derived-fuel-fired gas turbines was studied. Furnace oxidation behavior of plasma-deposited bond coatings was improved by increasing the thickness from 0.010 cm to 0.015 cm and by depositing the coatings at 20 kW with argon - 3.5-vol% hydrogen arc gas rather than at 11 kW with argon. The most oxidation resistant plasma-deposited bond coatings were Ni-14.1Cr-13.4Al-0.10Zr, Ni-14.3Cr-14.4Al-0.16Y, and Ni-15.8Cr-12.8Al-0.36Y on B-1900 + Hf and Ni-30.9Cr-11.1Al-0.48Y on MAR-M-509. The oxidation resistant bond coatings improved TBC life when the coatings were deposited on the specimens supported on a nail bed fixture during coating.

17. Key Words (Suggested by Author(s))	18. Distribution Statement
Thermal barriers Ceramic coatings Metallic coatings Burner rigs	Unclassified - unlimited STAR Category 26 DOE Category UC-90f

19. Security Classif. (of this report)	20. Security Classif. (of this page)	21. No. of Pages	22. Price*
Unclassified	Unclassified		

* For sale by the National Technical Information Service, Springfield, Virginia 22161